Documento de Trabajo 22/01

Hydroeconomic analysis of droughts in the Ebro basin using copulas for streamflow simulation

Daniel Crespo, Jose Albiac, Taher Kahil, Franziska Gaupp and Encarna Esteban

Unidad Trasversal de Economía Agroalimentaria
Centro de Investigación y Tecnología Agroalimentaria

CENTRO DE INVESTIGACIÓN Y TECNOLOGÍA AGROALIMENTARIA DE ARAGÓN

GOBIERNO DE ARAGON

Para obtener copias de este Documento de Trabajo, la información de contacto es:

José Albiac
Departamento de Análisis Económico
Universidad de Zaragoza
Gran Via 2
50005 Zaragoza
España

Correo electrónico: maella@unizar.es
Teléfono: +34 639958988

Este trabajo forma parte de los proyectos RTA2017-00082-00-00 "Sostenibilidad del Uso de la Tierra y el Agua en las Actividades Agrarias y Protección de los Ecosistemas ante las Sequías y el Cambio Climático" y RTA2014-00050-00-00 " La Gestión del Regadío ante la Escasez de Agua, las Sequias y el Cambio Climático" financiados en parte con fondos FEDER

Abstract

Climate change intensifies water scarcity in arid and semi-arid regions where pressures on water resources are significant, further compromising the sustainability of water systems. Climate change triggers more frequent, longer and intense droughts that bring about serious challenges for management. Hydroeconomic analysis provides a modeling framework for policy design at basin scale, taking into consideration the spatial and temporal relationships between water sectors. In this study, an integrated hydroeconomic model of the Ebro basin is used to analyze the economic impacts of climate change under several water management alternatives. An innovative approach, the Copula procedure, is used to generate longer, and more intense and frequent drought events. Several policy scenarios are simulated by combining two water allocation rules, proportional share or water markets, with the possibility of investments in advanced irrigation systems. The sustainability of the Ebro water system is evaluated by looking at its reliability, resilience and vulnerability under each policy alternative. The risk assessment of the benefit losses informs on the water system exposure to extreme drought events, and the contribution of management options in reducing potential losses. The results highlight that climate change exacerbates the likelihood of substantial economic losses from droughts, which compromise the sustainability of the water system. Water markets and irrigation efficiency enhancements reduce uncertainty and losses from droughts, although there is a trade-off between irrigation benefits and damages to aquatic ecosystems. However, the effectiveness of this policy combination decreases for longer and intense droughts.
Keywords: Hydro-economic model; climate change; drought impacts; water management; copula; drought intensity, duration and frequency

1. Introduction

Droughts are a natural hazard that impair the capacity of water systems to support economic activities (Borgomeo et al., 2015). Agriculture, natural ecosystems, hydropower, and urban and industrial supply are substantially exposed to water scarcity and can sustain significant economic losses (Naumann et al., 2015). Droughts and water scarcity are already a serious problem in arid and semiarid regions across the world, with increasing pressures from the impending climate change. In Europe, the evidence during recent years indicates that the drought anomaly in Europe is unprecedented in the past 2,000 years (Büntgen et al., 2021).[1]

Conflicts among users often arise from water scarcity, compounded by unsustainable management policies and lack of cooperation (Quiroga et al., 2011; Iglesias et al., 2007). The management challenge is serious because climate change widens the uncertainty of water planning (Herman et al., 2015; Sandoval-Solis et al., 2011) and the drought damages.

Costs of drought damages have been estimated at 9 billion € per year in the European Union (Cammalleri et al., 2020), and $8 billion per year in the United States (NOAA, 2021). These costs represent between 0.05% and 0.1% of the gross domestic product, although costs could be exceptionally higher some years. Kirby et al. (2014) estimate at 1% of GDP the costs of the 2009 drought in Australia, and Hernández et al. (2013) estimate the cost of the 2005 drought in the Ebro basin (Spain) at 0.5% of GDP.

The countries in Europe with large drought damages in billion € per year are Spain (1.5), Italy (1.4) and France (1.2), where drought planning efforts and climate adaptation actions are being developed. Most damages affect the agriculture (50%) and energy (35%) sectors, followed by the urban water supply sector (13%). Future damages would depend on the increase in the global warming temperature, with damages increasing up to five times for a +3°C scenario (Feyen et al., 2020).

Water management needs information to compare water system performance under a wide range of climate conditions in order to identify suitable governance alternatives. Sustainable water management faces the challenge of meeting human and environmental

[1] The anomaly seems to be driven by anthropogenic warming, which is changing the position of the summer jet stream.

water requirements while reducing the adverse impacts of droughts (Sandoval-Solis et al., 2011).

In Europe, drought frequency and intensity are highest in the Mediterranean area (Spinoni et al., 2015), with considerable damages sustained by Spain, France, Italy and Greece. Climate change will increase the frequency, intensity and duration of drought spells (IPCC, 2014). The effects would include reductions of crop and pasture production, higher risk of crop failures, livestock losses, land and ecosystems degradation, and negative impacts on hydropower and urban supply (Fallon and Betts, 2010; Li et al., 2009). Climate change will increase the vulnerability of water systems to droughts leading to critical failures, and the acute water scarcity will force adjustments in management to confront drought events (Vicente-Serrano et al., 2014; García-Ruiz et al., 2011).

The impact of droughts is driven by the intensity, duration and frequency of drought spells, and by the capacity of the system to endure these adverse events. River basin management policies should enhance the performance of the water system to confront disruptive events. Reliability, resilience and vulnerability are sustainability indicators that inform of the adequacy of management and policy alternatives.

Extreme droughts are climate events with low frequency, and they are rarely represented in climate projections (Rocheta et al., 2014). Water system vulnerabilities and management performance could be identified by generating synthetic stream flows that replicate historical and projected weather conditions.

Water management is challenging when drought spells entail large economic costs and environmental damages, especially in arid and semiarid regions. The difficulties of water management are compounded by economic growth, the increasing social concern for environmental protection, and climate change. This implies that water management becomes and adaptive process under constant revision based on updated information and knowledge. Hydroeconomic analysis (HEA) integrates biophysical, economic and ecosystem components in a framework that accounts for the temporal and spatial dimensions of water scarcity problems. Therefore, HEA is an important tool for evaluating water management adaptation to climate change (Ward 2021).

This paper analyzes the economic impacts of drought and water scarcity in the Ebro basin under alternative water allocation policies, taking into account that climate change results in more frequent, intense and longer droughts. The reliability, resilience and vulnerability of the water system to droughts are analyzed under different water management policies using HEA. An important innovation in this hydroeconomic modeling study is that the inflows in the model are generated using a statistical method denominated copula. This procedure generates more accurate streamflow series, which replicate historical stream flows and projected weather conditions with longer and more intense droughts.

2. Modeling framework

There is a wide variety of procedures to calculate runoff and streamflow from climate and environment variables, such as temperature, radiation, precipitation and vegetation cover. Drought studies use this information together with climate change scenarios, for enhancing the estimation of the intensity, duration and frequency of droughts. The statistical models used to model droughts could be based on regression analysis, variations of the autoregressive integrated moving average (ARIMA) model, Markov chains, artificial neural networks (ANN) or probabilistic characterization using copulas, among others (Mishra and Singh, 2011).

The approach taken in this study to drought modeling is to develop a model that can inform water management at basin level, with the objective of enhancing long-term water security. This requires an overall risk analysis as part of the selection of measures to be taken in drought planning. This study does not focus on the biophysical drought processes, but rather on the human-water interactions in the basin by looking at impact linkages and finding accurate representations of the human-water interactions (Brunner et al. 2020). This is in line with the essence of water systems analysis, which is the prediction of the hydrologic, socioeconomic and environmental consequences of water management (Brown et al., 2015).

The human-water interactions are represented using hydroeconomic modeling, which is a spatially and temporally distributed mathematical model, where water demand and supply nodes are characterized hydrologically and economically. This HEA approach could address the challenges faced by stakeholders in the management of water systems, because of the systematic integration of the hydrologic, engineering, economic, environmental and institutional dimensions of basins in a unique framework. The HEA framework has clear advantages in evaluating management and policy strategies for adaptation to climate change, by providing efficient water allocations across water uses, spatial locations, and time periods (Ward 2021).

The hydrological component of the model is represented by a simplified reduced form of the basin hydrology. Stream flows are stochastic, and therefore management decisions should be taken in a risk-based framework. Different risk metrics are used in water studies to compare the policy options for adaptation to climate change. Here we use the concepts of reliability (probability of failure), resiliency (recovery duration) and vulnerability (failure damages) for water system performance, which were proposed by Hashimoto et al. (1982).

Modeling the hydrology requires the consideration of the joint distribution of random variables, and we use the copula procedure to generate the headwaters entering the hydrological network. The advantage of the copula approach is that the dependence between the variables is independent from the choice of the marginal distributions of individual variables.

Generating synthetic stream flows overcomes the constraints imposed by the lack of long series of historical information. Streamflow generation is important in hydrology studies, and estimation methods cover a broad range of techniques. Representing extreme values using multivariate analysis is uncommon because of the limited number of multivariate distributions that represent extreme values. Distributions like bivariate Pareto and bivariate Gamma distributions could represent extreme values of two random variables. The problems with those distributions are that: the same distribution is needed for each marginal distribution; the estimation of parameter for these distributions could be difficult; and the extension to more than two variables are problematic.

The copula approach resolves these problems because the marginal distributions are fitted independently, parameters are estimated by maximum likelihood, and extensions to more than two variables are straightforward by regular and canonical copulas. The univariate marginal distributions and the multivariate dependence structure are separated, with the marginal distributions fitted independently and the dependence structure represented by a copula. Compared to other methods of streamflow simulation, copulas are flexible in the selection of marginal distributions, the dependence structure of variables, and the extension to multiple variables (Chen et al., 2015).

2.1 Streamflow simulation methodology

Duration, frequency and intensity are temporal variables that characterize droughts. Monthly stream flows are stochastic variables with temporal dependence, and the drought persistence is driven by this temporal dependence. Here the objective is to generate streamflow series matching the behavior of historic data but capable of including the climate change effects on droughts' intensity and duration. Several methods are used to simulate stream flows, such as autoregressive moving average, block bootstrapping, Markov chain processes, and copulas. The copula-based method is gaining traction to characterize the joint probability distributions of stream flows, and droughts with longer duration and larger intensity than previously observed can be generated by perturbing the copula parameter (Borgomeo et al., 2015; Salvadori and De Michele, 2004).

Monthly streamflow X_m in month m is a stochastic variable with a cumulative distribution function (cdf) $F(X_m)$. The probability integral transform states that $u_m = F(x_m) = P(X_m \leq x_m)$, where u_m has the standard uniform distribution. Two consecutive monthly stream flows are correlated and their dependence is represented by the joint cdf $H_{x_{m-1},x_m}(x_{m-1}, x_m) = P(X_{m-1} \leq x_{m-1}, X_m \leq x_m)$, where the marginal cumulative distributions of $H_{x_{m-1},x_m}(x_{m-1}, x_m)$ are $u_{m-1} = F_{m-1}(x_{m-1})$ and $u_m = F_m(x_m)$. Standard multivariate modeling is a complex task that may not yield the best fit for hydrological variables, and the copula-based method can overcome the difficulties in modeling multivariate distributions.

The copula is a function that links univariate cumulative distributions to create a multivariate distribution function. A copula is a joint distribution of two uniform random variables, and the Sklar's theorem states that the joint distribution function $H_{x_{m-1},x_m}(x_{m-1}, x_m)$ can be expressed in terms of their marginal distributions $F_{m-1}(x_{m-1})$ and $F_m(x_m)$, by defining a copula C as:

$$H_{x_{m-1},x_m}(x_{m-1}, x_m) = C\big(F_{m-1}(x_{m-1}), F_m(x_m)\big) = C(u_{m-1}, u_m)$$

where $C: [0,1]^2 \rightarrow [0,1]$ denotes the copula function, and $C(u_{m-1}, u_m) = Pr[U_{m-1} \leq u_{m-1}, U_m \leq u_m]$. The copula captures the dependence of two consecutive months. In order to generate random values of stream flows, the conditional distribution method was used in this study. The conditional probability of flow x_m given the flow at x_{m-1}, $Pr(X_m \leq x_m | X_{m-1} = x_{m-1})$, can be obtained from the copula as:

$$t = H_{x_{m-1},x_m}(x_m|x_{m-1}) = P(U_m \le u_m|U_{m-1} = u_{m-1}) = C(u_m|u_{m-1}) = \frac{\partial C(u_{m-1}, u_m)}{\partial u_{m-1}}$$

This relationship feeds the simulations of the correlated random variables. If the flow at month $m-1$ is known, the value of u_{m-1} is given by evaluating $F_{m-1(x_{m-1})}$. Then, the value of u_m can be simulated from the inverse function $C^{-1}(u_m\ |u_{m-1})$ and a uniform random number t. The flow at month m is obtained from the inverse function or quantile function F_m^{-1} as $x_m = F_m^{-1}(u_m)$.

To simulate monthly stream flows, the distribution function of monthly stream flows and the copula have to be fitted. There are several distribution functions to model monthly streamflow, and the usual distribution functions are employed for characterizing hydrological variables. The Clayton copula is selected in this study for modeling droughts because it characterizes variables with low tail correlation, such as droughts.

The monthly streamflow is a random variable with unknown distribution function. The distribution functions tested to fit the marginals of the copulas were Gamma, Lognormal, Weibull, Pearson III and Generalized Extreme Values. The Lognormal, Pearson III and GEV distributions have been selected to represent the marginals of the copula. The parameter of the distributions is estimated maximizing the likelihood function of the density function. The goodness of fit is computed by the Kolmogorov-Smirnov (KS), Anderson-Darling (AD) and Cramer-Von Mises (CVM) tests, which identify the distribution that better fits the observed data. Finally, the distribution is selected comparing the Bayesian and Akaike information criteria (BIC and AIC).

There are many types of copula structures C. The Archimedean copulas are a family of copulas commonly used to describe different correlation structures between variables. The copula considered in this study is the Clayton copula of the Archimedean copula family. The Archimedean copulas are defined as follows:

$$C(u_{m-1}, u_m) = \varphi^{-1}[\varphi(u_m) + \varphi(u_{m-1})]$$

where φ is the generator function that is a strictly decreasing function from $[0,1]$ onto $[0, \infty]$. The Clayton copula of two consecutive months is defined as:

$$C(u_{m-1}, u_m) = \left[u_{m-1}^{-\theta} + u_m^{-\theta} - 1\right]^{\left(\frac{-1}{\theta}\right)}$$

Figure 1. Streamflow simulation procedure based on Copulas

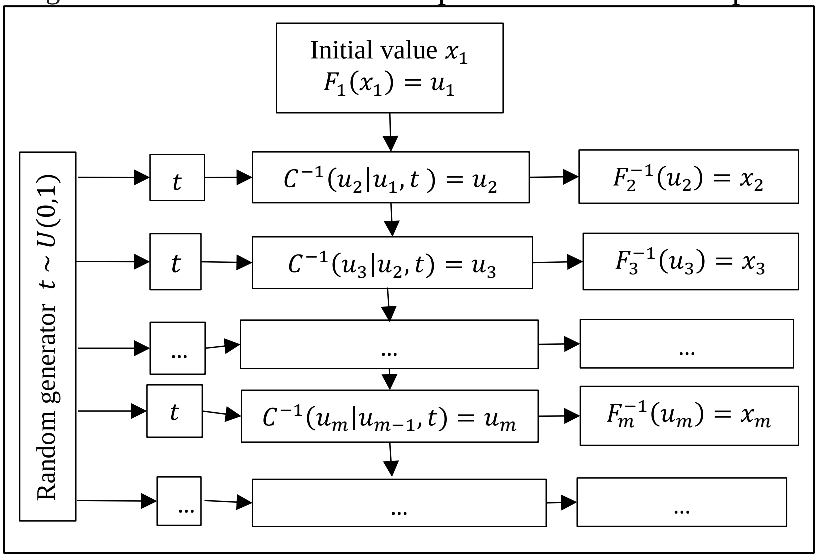

The conditional distribution of the Clayton copula is expressed as:

$$t = P(U_m \leq u_m | U_{m-1} = u_{m-1}) = \frac{\partial C(u_{m-1}, u_m)}{\partial u_{m-1}}$$

$$= u_{m-1}^{-(\theta+1)} \left(u_{m-1}^{-\theta} + u_m^{-\theta} - 1\right)^{-\left(\frac{1+\theta}{\theta}\right)}$$

and the inverse function of the conditional distribution of the Clayton copula is:

$$u_m = \left[1 + u_{m-1}^{-\theta} \left(t^{\left(-\frac{\theta}{1+\theta}\right)} - 1\right)\right]^{\frac{-1}{\theta}}$$

Figure 1 shows the procedure followed for simulation. If the streamflow X_{m-1} at month $m - 1$ is known, it is possible to simulate the streamflow at month m using the inverse function of the conditional distribution. The first step is to obtain the value of u_{m-1} using the cdf $F_{\mathrm{m}-1}(x_{m-1}) = u_{m-1}$, and then a uniform random number t between zero and one is generated. The second step is to find u_m using the inverse function of the conditional distribution of the copula. The value of the simulated flow x_m is obtained with the inverse function of the cdf $F_m(x_m)$.

The simulation of the monthly stream flow using conditional copulas are summarized as follows

1) Fit the marginal distribution $F_m(x_m)$ for each month $m = 1,2, \dots ,12$.
2) Fit the joint distribution using copulas for each pair of months and estimate their parameters θ_i where $i = 1,2, \dots ,12$.

$$C\big(F_1(x_1), F_2(x_2)\big), \dots, C\big(F_{m-1}(x_{m-1}), F_m(x_m)\big), \dots, C\big(F_{12}(x_{12}), F_1(x_1)\big)$$

3) Given the streamflow x_{m-1} in month $m-1$, u_{m-1} can be calculated with the marginal $u_{m-1} = F_{m-1}(x_{m-1})$. A uniform random variable t between zero and one is generated, and the value of u_m is obtained from the inverse conditional function.
4) The value of the streamflow at month m is calculated with the inverse distribution function $x_m = F_m^{-1}(u_m)$

The copula simulation procedure can be used to simulate longer droughts by multiplying the parameter of the copula θ_i by a factor β, where the values one, two, six and ten are selected for factor β. For each perturbation of β, 1.000 sequences were generated using the conditional method described before. The streamflow generation method has been used to generate 40 years of monthly stream flows.

2.2 Model components and scenarios

The hydroeconomic model of the Ebro basin integrates hydrological, economic, environmental and institutional aspects. The model includes a reduced-form hydrological model, a regional economy component, and an environmental benefit component.

2.2.1 Reduced-form hydrological component

The hydrological component represents flows between supply and demand nodes, using the hydrological principles of water mass balance and flow continuity in the river. The hydrological component shows the spatial distribution of water flows used by economic sectors and environmental flows. The mathematical formulation is as follows:

$$W_{out_d,m,y} = W_{in_d,m,y} + W^{res}_{rel_d,m,y} - W_{loss_{d,m,y}} - Div^{IR}_{d,m,y} - Div^{URB}_{d,m,y} \tag{1}$$

$$W_{in_{d+1},m,y} = W_{out_d,m,y} + r_d^{RI} \cdot \left(Div^{IR}_{d,m,y}\right) + r_d^{URB} \cdot \left(Div^{URB}_{d,m,y}\right) + \\ + RO_{d+1,\mathrm{m,y}} \tag{2}$$

$$W_{out_{mouth},m,y} \geq E_m^{min} \tag{3}$$

Equation (1) is the mass balance equation, and it determines water outflow $W_{out_d,m,y}$ in river reach d, in year y and month m, which is equal to water inflow $W_{in_d,m,y}$, plus water release $W^{res}_{rel_d,m,y}$ from reservoir res, minus water losses $W_{loss_{d,m,y}}$, water abstraction for irrigation $Div^{IR}_{d,m,y}$, and abstraction for urban and industrial use $Div^{URB}_{d,m,y}$.

Equation (2) guarantees river flow continuity, in which water inflow in the following river reach $W_{in_{d+1},m,y}$ is the sum of the water outflow from the previous reach $W_{out_{d},m,y}$, return flows from previous irrigation districts $\left[r_d^{RI} \cdot \left(Div_{d,m,y}^{IR}\right)\right]$, urban return flows $[r_{d,m,y}^{URB} \cdot \left(Div_{d,m,y}^{URB}\right)]$, and flows entering this river reach from tributaries $RO_{d+1,m,y}$. Equation (3) states that water outflow at the mouth of the Ebro $W_{out_{mouth},m,y}$ must be above the minimum environmental flow level.

The model dynamics is driven by the water storage in reservoirs. The formulation of the reservoirs' storage is as follows:

$$Z_{res,m,y} = Z_{res,m-1,y} - W_{rel_d,m,y}^{res} - W_{evp,m,y}^{res} \tag{4}$$

$$Z_{res,0} = B_{res,0} \tag{5}$$

$$Z_{res,t} \leq C_{res}^{max} \tag{6}$$

$$Z_{res,t} \geq C_{res}^{min} \tag{7}$$

$$W_{evp,m,y}^{res} = Evp_{res}\, S_{res,m,y} \tag{8}$$

$$S_{res,m,y} = \alpha_{res} + \beta_{res}\, Z_{res,m,y} \tag{9}$$

Equation (4) states that the reservoir stored water $Z_{res,m,y}$ is equal to the stock in the previous period, $Z_{res,m-1,y}$, minus both net release (outflow minus inflow), $W_{rel_d,m,y}^{res}$, and evaporation, $W_{evp,m,y}^{res}$. Equation (5) is the initial reservoir water stock at $m = 12$ and $y = 0$, $B_{res,0}$. Equations (6) and (7) are upper and lower bounds on reservoir storage, given by maximum capacity, C_{res}^{max}, and dead storage C_{res}^{min}. Equation (8) states that reservoir evaporation, $W_{evp,m,y}^{res}$, is proportional to the reservoir surface area, $S_{res,m,y}$. The parameter Evp_{res} is the water evaporation per hectare of reservoir surface area (Mm^3/ha). Equation (9) states the linear relationship between reservoir surface area and stored water, where parameters α_{res} and β_{res} are the intercept and the linear coefficients of the surface-storage equation. This equation gives a good approximation because storage variations are limited between the upper and lower bounds.

The hydrological component has been calibrated introducing auxiliary variables for river reaches, so that so that the predicted gauged flows are broadly consistent with observed flows at each river gauge where measurement data are available. Calibration is used to close the mass balance equation, since there are water inflows and outflows in the system that cannot be observed (for example, underground flows, evaporation, or some return flows). Calibration includes non-observed flows, which are the difference between flows estimated with the model and flows measured at gauging stations. The parameters of the surface-storage equation are obtained using the database in Yigzaw et al. (2018).

2.2.2 Regional economic component

The regional economic component includes agricultural irrigation and urban water use. There is an optimization model for agricultural activities in every irrigation district, which maximizes farmers' private benefits from crop production subject to technical and resource constraints. Crop yield functions are assumed linear and decreasing in cropland acreage, and output and input prices are constant. The optimization problem is formulated as follows:

$$Max\left(B_{k,y}^{IR}\right) = \sum_{ij} C'_{i,j,k} \cdot X_{i,j,k,y} \quad (10)$$

s.t.

$$\sum_{i} X_{i,j,y} \leq T_{land_{k,j}};\ j = flood, sprinkler, drip \quad (11)$$

$$\sum_{ij} W_{i,j,k,m} \cdot X_{i,j,k,y} <= T_{water_{k,m,y}} \quad (12)$$

$$\sum_{ij} M_{i,j,k} \cdot X_{i,j,k,y} \leq T_{la_k} \quad (13)$$

$$X_{per,j,k,y} \leq X_{per,j,k,y-1} \quad (14)$$

$$X_{i,j,k,y} \geq 0 \quad (15)$$

where $B_{k,y}^{IR}$ is private benefit in irrigation district k and year y, and $C'_{i,j,k,y}$ is net income of crop i using irrigation technology j. The decision variable of the optimization problem is $X_{i,j,k,y}$, which is acreage of crop i under irrigation technology j, in year y. Equation (11) represents the restriction of available land $T_{land_{k,j}}$ in irrigation district k equipped with irrigation system j. Equation (12) states that water applied in an irrigation district k, in year y and month m, is restricted to water availability $T_{water_{k,m,y}}$, where $W_{i,j,k,m}$ is the water requirement of crop i with technology j, in month m. The water available $T_{water_{k,m,y}}$ in irrigation district in year at month m is the variable linking the optimization model of irrigation districts and the hydrological component. The labor constraint (13) represents labor availability T_{la_k} in irrigation district k, where M_{ijk} is the labor requirement of crop i with irrigation system j. Equation (14) states that fruit trees for each irrigation district, at year y, cannot exceed the fruit trees irrigated the previous year, $y - 1$. This constraint represent future loss of capital investment in fruit trees if farmers decide not to irrigate in the current time period.

This optimization model includes the major crops in every irrigation district. Irrigation systems for field crops are flood and sprinkler, and for fruit trees and vegetables the irrigation systems are drip and flood. Net income per hectare C'_{ijk} is the difference between crop revenue and direct and indirect costs (including capital amortization) and it is expressed by $C'_{ijk} = P_i Y_{ijk} - CP_i$ where P_i is price of crop i, Y_{ijk} is yield of crop i under technology j in the irrigation district k, and CP_i are direct and indirect costs of crop i (including water costs).

The crop yield function is linear and represents decreasing crop yields when additional land is assigned to crop production, based on the principle of Ricardian rent. The first lands in production have the highest yields, and yields fall off as less-suitable lands enter production. The crop function relates yields with acreage of crop i under irrigation technology j, and is defined as:

$$\mathrm{Y_{ijk}} = \beta_{0_{\mathrm{ijk}}} + \beta_{\mathrm{1ijk}} \mathrm{X_{ijk}} \qquad (16)$$

The agricultural component is calibrated using the Positive mathematical programming (PMP) to reproduce the observed land and water use under baseline conditions, and to address the problem of crop overspecialization (Howitt 1995). Calibration follows the PMP procedure by Dagnino and Ward (2012), where parameters are estimated for a linear yield function [Equation (16)] based on the first-order conditions of benefit maximization. Data on yields, prices, crop water requirements, production costs, availability of water resources, land and labor, together with information on biophysical parameters have been obtained from statistical databases, reports, previous studies and expert consultation (MARM, 2010; MAGRAMA, 2015; INE, 2009; DGA, 2009; GC, 2009; GN, 2009).

The modeling of urban water maximizes economic surplus, the sum of consumer and producer surpluses in the basin's main cities. The optimization problem of the urban sector is expressed by:

$$MaxB_{u,y}^{URB} = \left(a_{du} Q_{du,y} - ½\, b_{du} Q_{du,y}^2 - a_{su} Q_{su,y} - ½\, b_{su} Q_{su,y}^2\right) \qquad (17)$$

s.t.

$$Q_{du,y} - Q_{su,y} \leq 0 \tag{18}$$

$$Q_{du,y};\ Q_{su,y} \geq 0 \tag{19}$$

where B_u^{URB} is the consumer and producer surplus in city u. The variables $Q_{su,y}$ and $Q_{du,y}$ are water supply and demand in city u, respectively. The parameters a_{du} and b_{du} are the constant term and the slope of the inverse demand function, and the parameters a_{su} and b_{su} are the constant term and the slope of the water supply function. Equation (17) states that the supply must be equal to or greater than the demand for water. The water supply $Q_{su,y}$ is the variable linking urban water with the hydrological component. The equation parameters have been obtained from the studies by Arbués et al. (2004) and (all unit prices are expressed in euros at 2009).

2.2.3 Model optimization, scenarios and sustainability outcomes

The net present value (NPV) of the benefits of economic sectors is maximized over the planning horizon, where NPV is the sum of present benefits from agricultural irrigation and urban water use. The model optimizes the objective function:

$$Max\ NPV = \sum_{k,y} \frac{B_{k,y}^{IR}}{(1+r)^y} + \sum_{u,y} \frac{B_{u,y}^{URB}}{(1+r)^y} \tag{20}$$

subject to the basin's hydrological, land use, institutional, and environmental constrains stated in equations (1) to (19).

The performance of the Ebro water system will be threatened by climate change and the increasing frequency, duration and intensity of droughts. Several indicators such as reliability, resilience or vulnerability are used to assess water system performance to disruptive events like droughts. Reliability is the probability that water supply could meet water demand during the simulation period, where reliability is simply one minus the risk of system failure. Resiliency describes the capacity of the system to recover after a system failure, and vulnerability can be measured by the economic losses of drought spells.

Sustainability and risk-based indicators contribute to the assessment of the likelihood and impact of disruptive events on water systems. A comprehensive sustainability index can be built by combining reliability, resilience and vulnerability indicators in a general sustainability index. This sustainability index is used in the Ebro to compare the performance of the water system under different management and policy strategies for climate change adaptation.

The analysis of the impact of water scarcity on the sustainability of the water system is undertaken under several scenarios, which combine climate change conditions, water allocation policies, and investments in advanced irrigation systems.

The assumptions for climate change in the Ebro for the next 40 years simulation period are the following: the mean inflows in the basin decline progressively up to 12%, and higher temperatures increase crop evapotranspiration and dam evaporation by 5.7% and 6%, respectively. Climate change will also increase drought persistence, with longer droughts spells. The copula procedure is used to account for the longer duration of droughts. Ten inflow series of forty-year each have been simulated by the copula for a given value of parameter θ, which regulates drought duration. The duration of historical droughts are represented by parameter θ, and then the parameter is increased to 2θ, 6θ and 10θ to represent longer drought durations.

There are three climate scenarios: 1) current climate, which replicates historical inflows, temperature, and drought duration; 2) future climate with decreasing inflows, increasing temperature, and historical drought duration; and 3) future climate with decreasing inflows, increasing temperature, and longer drought duration. Scenarios 2 and 3 compare future climate with historical or with longer drought duration, and the reason is to discern the effects of drought duration and intensity.

The water allocation policies analyzed are institutional cooperation and water markets. Institutional cooperation is the current policy applied by the water authority in the Ebro basin. Under drought conditions, the basin authority reduces water allocations for irrigation in relation to drought intensity, assigning the fall of inflows by proportional share. Under the water markets policy, farmers receive the water allocations of institutional cooperation, but then these water allocations can be exchanged among irrigation districts, maximizing the private benefits of water use. There is no direct exchange of water between selling and buying irrigation districts, but rather the selling district reduces withdrawals and the buying district augments withdrawals in their respective river reaches.

Table 1. Climate change, water allocation and efficiency investment scenarios.

Climate change conditions		**Water allocation policy**	**Efficiency investments**
No climate change		*Proportional share*	*No efficiency enhancements*
Inflows			
Parameter θ does not change. Inflows and drought spells replicate historical behavior. Mean inflows are the observed levels	Crop evapotranspiration and dam evaporation do not change	Under drought, water allocations for irrigation are reduced in proportion to drought intensity	Irrigation technology does not change, with channel efficiency between 70% and 90%
Climate change		*Water markets*	*Efficiency enhancements*
Inflows			
Drought duration is prolonged by increasing the copula parameter θ. Stream flows are simulated for 2θ, 6θ and 10θ. Inflows fall steadily up to 12% in 2040	Crop evapotranspiration and dam evaporation increase up to 5.7 and 6% in 2040, respectively.	Water is exchanged among irrigation districts Water is exchanged among irrigation districts	More efficient irrigation technologies. Irrigation systems change to sprinkle for field crops (except rice), and drip for fruit trees and vegetables. Channel efficiency is also increased

The investments in advanced irrigation systems is the preferred solution by decision makers to confront water scarcity in most arid and semiarid basins around the world. These investments improve the water conveyance systems and the irrigation equipment in parcels, with gains in water efficiency at irrigation district level and higher crop yields. However, Grafton et al. (2018) indicate that these investments tend to reduce stream flows in basins, and call it "the paradox of irrigation efficiency". Channel efficiency in the Ebro range between 70% and 90% at present, and investments improve all channels up to 90% efficiency. Current parcel irrigation technologies include flood, sprinkle and drip irrigation, and investments will expand in the basin sprinkle irrigation to all field crops (except rice), and drip irrigation to all vegetable and fruit crops.[2] Table 1 summarizes the main aspects of the simulated scenarios.

3. Results

The results correspond to each combination of climate change and policy scenarios, by performing eleven series of forty-year length simulations. These simulations are replicated with the data on water inflows that are generated for the different values of the factor β in the copula procedure (β=1, 2, 6 and 10), which regulate drought duration.

[2] The investment costs of these advanced irrigation technologies are included in the benefits of crops.

Figure 2. Expected irrigation area under climate and policy scenario (10^3 ha)

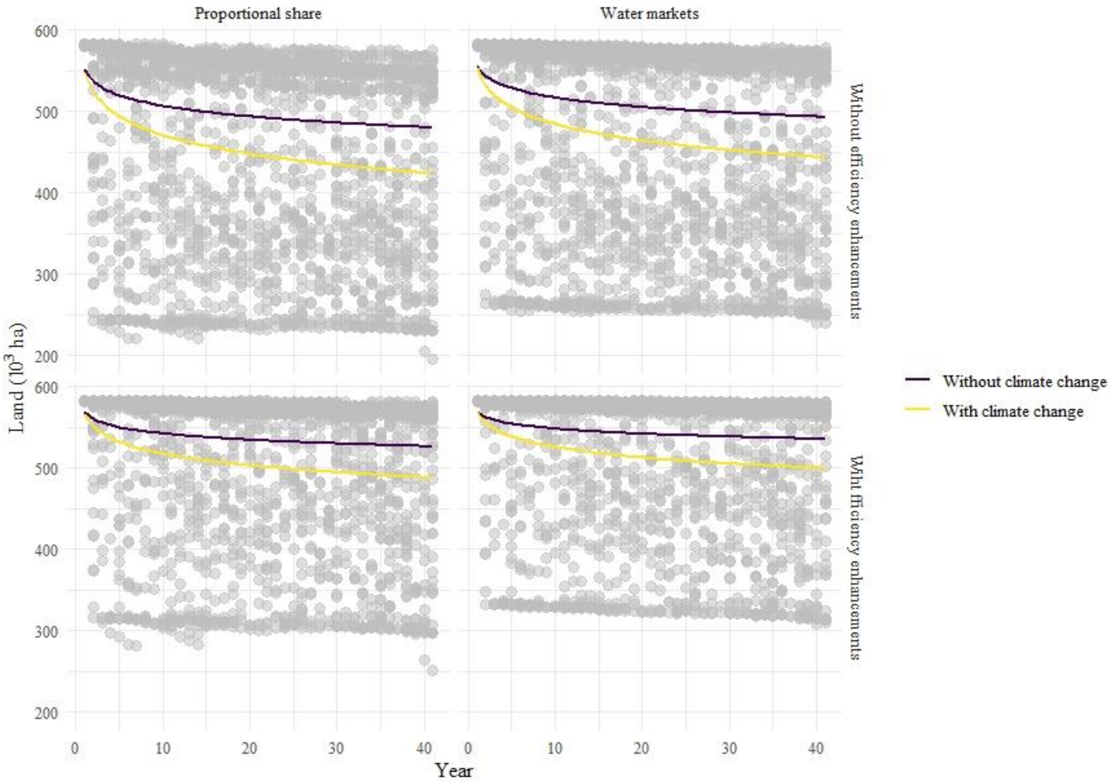

Then, the outcomes from each combination of policies are calculated. The results show the impacts of droughts on irrigated cropland, water extractions and irrigation benefits.

The analysis in irrigation districts shows the adaption strategies in cropland distribution undertaken by districts. Simulations provide monthly information on water withdrawals, environmental stream flows, water scarcity, and water system stress. The information is used to estimate reliability, resilience, vulnerability and sustainability indicators, which reveal the system performance.

3.1 Sustainability of the water systems for irrigation

Drought intensity and duration generate benefit losses, which indicate the system sensibility to drought events. The performance of the different policies is compared, in order to identify which are the tradeoffs between policies.

Figure 3. Annual cropland distribution under climate and policy scenarios (10^3 ha)

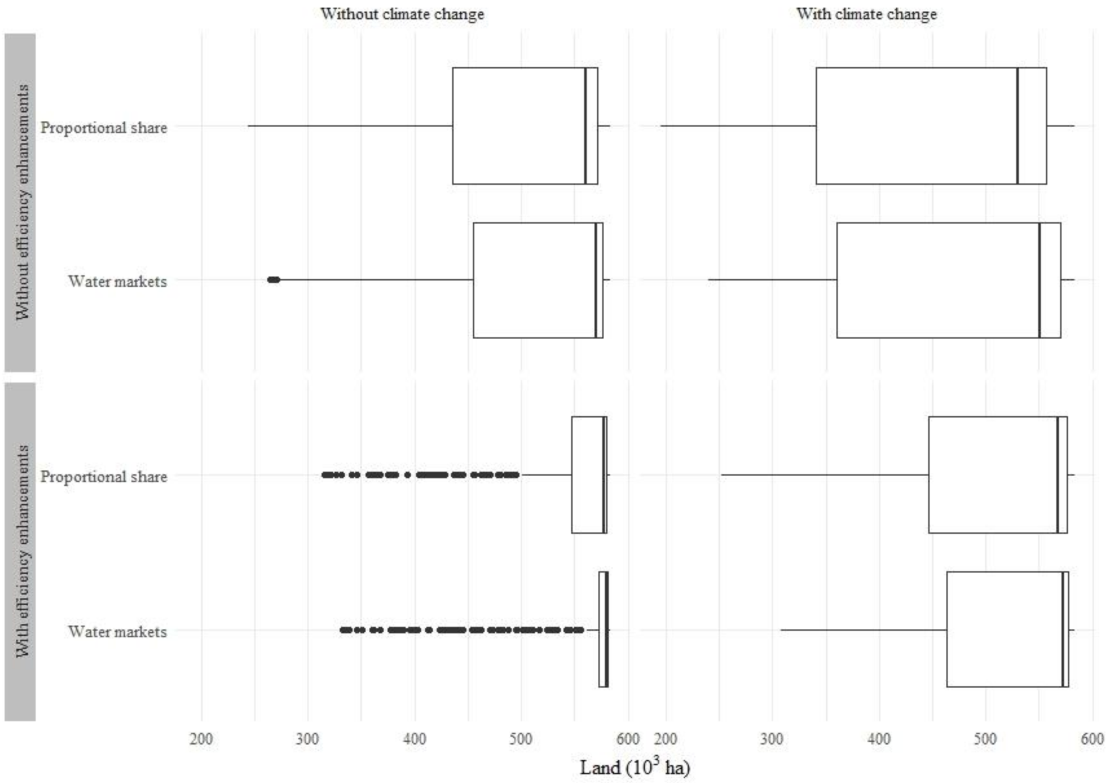

In figure 2, the grey points display the irrigated area by year for climate change and policy scenarios. The lines are smoothed trends, assuming a logarithmic relationship between irrigated area and time. The top panels show the irrigated area with and without climate change, for water markets (top-left) and proportional share (top-right) policies under current irrigation technologies. The bottom panels show the irrigated area for improved irrigation technologies. The irrigated area declines in the future because of the recurrent drought events and the growing trend in water scarcity from climate change.

Annual cropland, water diversions and benefits under climate and policy scenarios, are presented in figures 3, 4 and 5, respectively. The size of boxplots range between the first and third quartiles of the distribution, providing information on dispersion and uncertainty. The first quantile indicates the 25% of worst cases or the 75% of best cases.

Climate change exacerbates water scarcity problems, worsening the drought impacts. Enhancements in the efficiency of parcel irrigation systems and conveyance channels contributes to moderate the fall in irrigated cropland. The efficiency enhancements contribute to meet the water consumed by crops, especially under climate change when crop water requirements increase. The water market policy slows down cropland reductions, compared with the proportional share policy. The combination of water markets and efficiency enhancements maintains more cropland in production, but also

Figure 4. Annual water diversions distribution by climate and policy scenarios (Mm^3).

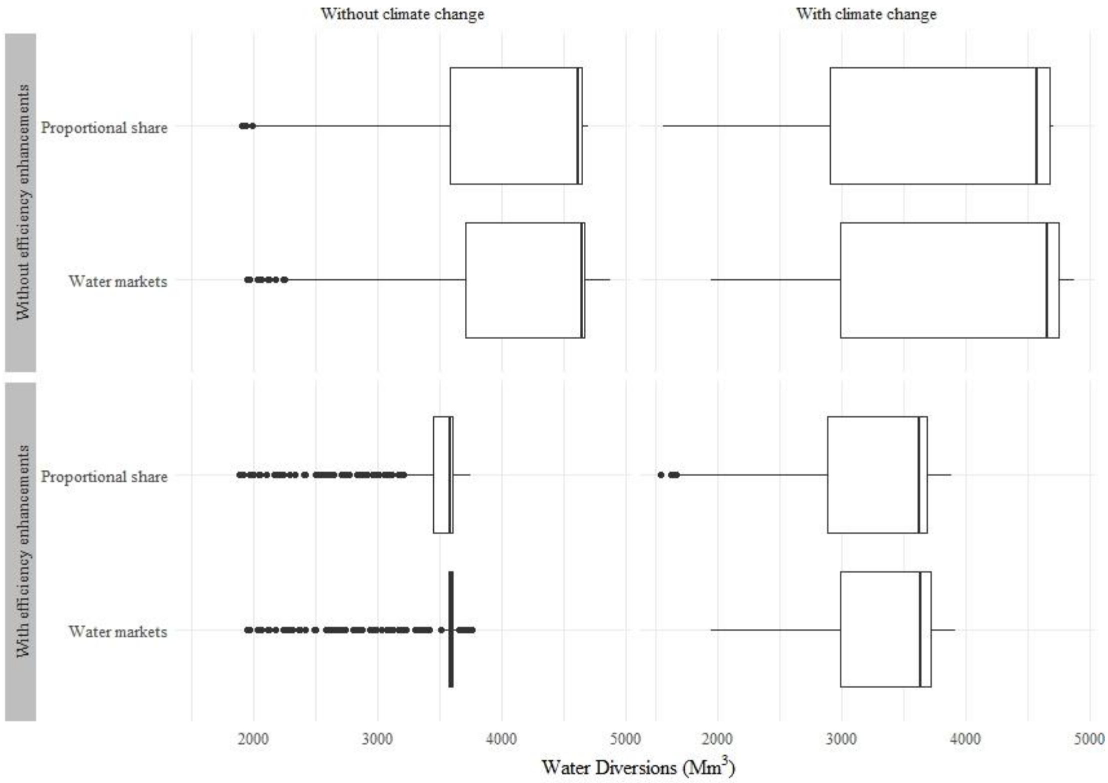

shrinks environmental flows. Under climate change, the first quartile of irrigated area is around 100.000 ha lower for all policy scenarios.

The vertical line dividing the boxplots is the median of the cropland distribution ranging between 525,000 and 580,000 ha for all scenarios (figure 3), with the median close to the baseline irrigated area (580,000 ha). Normal or wet weather conditions occur in half of the time periods, during which the baseline crop production and water extractions are maintained.

The impact of droughts is determinate by several factors like water stored in dams, monthly inflows and policy. The relationship between irrigated area reductions and annual water inflows is estimated by a Beta regression (see table A1 in the appendix for details). Regression parameters are used to estimate the expected land reduction under alternative policies. For example, investments in efficiency enhancement cut by half land reductions, compared with maintaining current irrigation efficiency (Table A1).

Table 2. Percentage cropland reduction over the baseline, under climate change and policy.

		First period of the simulation		*Last period of the simulation*	
		Moderate drought (-15%)	Extreme drought (-50%)	Moderate drought (-15%)	Extreme drought (-50%)
Without climate change	*Without efficiency enhancements*				
	Proportional share	8.40%	33.40%	19.10%	56.20%
	Water markets	6.90%	28.60%	15.90%	50.70%
	With efficiency enhancements				
	Proportional share	4.00%	18.60%	9.70%	36.80%
	Water markets	3.30%	15.50%	7.90%	31.80%
With climate change	*Without efficiency enhancements*				
	Proportional share	9.10%	35.20%	20.40%	58.10%
	Water markets	7.40%	30.30%	17.00%	52.70%
	With efficiency enhancements				
	Proportional share	4.40%	19.80%	10.40%	38.70%
	Water markets	3.50%	16.50%	8.50%	33.60%

The drought scenarios are moderate drought where water inflows fall by 15% and extreme drought where water inflows fall by 50%. Table 2 presents the policy results from the beta regression predictions. The percentages indicate the expected land reductions under moderate and extreme drought conditions, for the first and last periods of simulation. Results show that under the same policy and climate condition, the fall in irrigated area doubles between the first and last periods. Climate change increases land reduction between one and two percentage points. The mitigation capacity of the combined policies declines with drought severity, climate change and time. The market policy cuts the reduction in cropland by 20%, compared with the proportional policy, while investments in irrigation efficiency cut cropland reductions by 55% compared with no investments (Figure A4 and table 1 in the appendix).

The response of farmers to drought is reducing field crops and maintaining fruit trees and vegetables. Corn represents around 18% of total crop mix and remains constant under drought conditions, while the other field crops fall. Wheat and rice acreage diminish progressively until they get out of production. Fruit trees and vegetables share of crop mix grow, in particular vineyard and peach. Five crops account for 75% of the irrigated area in the baseline, but under drought the cropping pattern is more diversified and

Figure 5. Annual benefits distribution under climate and policy scenarios (10^6 €).

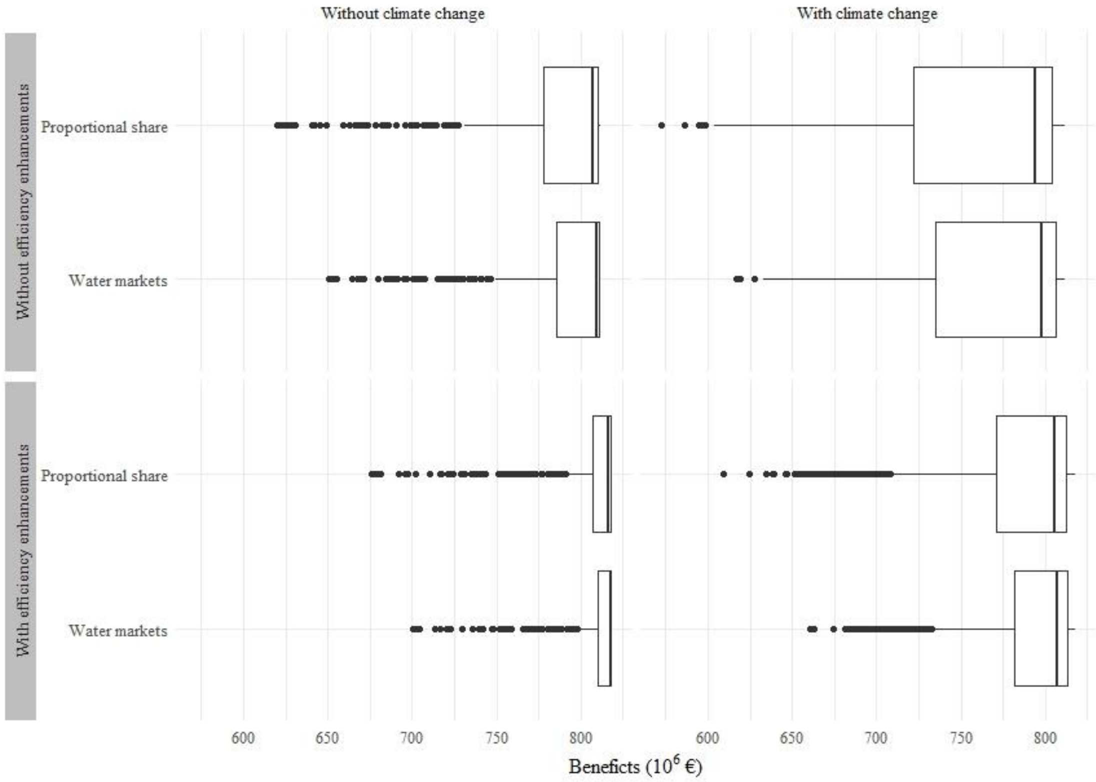

minority crops gain importance (Figure A5 and figure A6 in appendix). Adaptation to drought involves the retirement of crops with high water consumption and low profitability.

Water scarcity takes place during droughts, and their impact depends on the policy mix that combines proportional share or water markets, with current or enhanced water efficiency. Stream flows lower than the median correspond to 50% of the worst cropland reductions, and the ensuing likelihood and size of benefit losses. Water extractions are driven by climate conditions and policies. The enhancement of irrigation systems reduces water extractions from 4,500 Mm^3 to 3,500 Mm^3 under normal weather, where basin inflows are around the historic mean (Figure 4).

Climate change increases water diversions because of the rising temperatures and evaporation, even under normal and wet weather conditions. Also, the likelihood of water scarcity and droughts increases under climate change, which shrinks mean inflows and enlarges the duration of drought spells. Under climate change, the first quartile of water diversions is around 3,000 Mm^3 for all policy scenarios, which shows the fall of water in the basin when droughts are severe.

Table 3. Min, 1st quartile, mean, median, 3rd quartile and max of annual benefits under drought by policy-mix.

	Min	1st Quartile	Mean	Median	3rd Quartile	Max
Without efficiency enhancements						
Proportional share	573	729	762	797	806	812
Water markets	617	741	769	800	808	812
With efficiency enhancements						
Proportional share	609	776	785	808	814	818
Water markets	660	786	791	809	815	818

The index of water stress is the proportion of water diversions over water inflows, so the water deficit is the gap between water diversions and water inflows. Water scarcity and water stress are especially intense in summer, when crop water requirements are large and water inflows small, demonstrating the importance of dams to meet water demand. Water stress is more likely from June to September when water extractions double basin inflows, and the water system could be in stress (Figure A7 in appendix). However, water stress and water scarcity can be underestimated because environmental flows are not included in the supply-demand balance.

Larger irrigated cropland involves more water extractions and consumption (evapotranspiration), reducing stream flows in the basin. Under drought, investments in irrigation efficiency increase water extractions by 25% to 30% in comparison with maintaining current irrigation efficiency (Figure A8). The consequence is lower stream flows at the river mouth, with an average fall around 200 Mm^3 (Figure A9).

The annual benefits for policy and climate scenarios are presented in Figure 5. The median benefits are close to baseline benefits (820 M€), and range between 790 and 820 M€. To assess the effects of climate change on the distribution of benefits, we have pooled the data of benefits from all policy scenarios, Climate change displaces the distribution of benefits, since without climate change the benefits exceed 775 M€ in 75% of the cases, but with climate change the benefits exceed only 725 M€ in 75% of the cases.

Weather conditions are stochastic, and therefore the impacts of drought are also stochastic. These impacts are measured by the benefits obtained under each combination of policies. Then, the benefit outcomes from each combination of policies are compared. The first quartile of the distribution of benefit contains the worst benefit outcomes from drought events. Also, climate change amplifies the dispersion of benefits, while increasing both the uncertainty and likelihood of the fall in benefits.

Table 3 shows the minimum, first quartile, mean, median, third quartile and maximum of the annual benefits by policy mix, which combines proportional share or water markets, and current or enhanced water efficiency. Benefits are higher for water markets compared to proportional share, and benefits are also higher for efficiency enhancements compared to current efficiency. The mean benefits fall from 820 M€ of the baseline scenario to between 760 and 790 M€, depending of the policy combination.

The likelihood and size of benefit losses from drought impacts reveal the degree of exposure of the water system to adverse events. Risk is measured by the probability (likelihood) of withstanding a certain level of benefit damages (size), and risk management plays an important role in decision making. Value at risk (VaR) is a standard risk measure that calculates the benefit level that is not exceeded for a given probability or confidence interval. VaR can also be calculated in terms of benefit losses by the exceedance of probability, which is the probability of exceeding a certain benefit loss. Therefore, in terms of benefits losses, VaR is the benefit loss that is exceeded for a given probability or confidence interval (see section 3 of the appendix for details).

The VaR for a 5% probability is widely used for risk assessment, and the combination of water markets and efficiency enhancements reduce in 70 M€ the benefit loss level of the VaR at 5%, compared with proportional share and current irrigation efficiency. This reduction in benefit losses represent around 8% of baseline benefits (Figure A10). Figure 6 shows the results by irrigation district of the mean percentage reductions from the baseline scenario of variables benefits, water diversions, labor, cropland, and cultivated areas of field trees, field crops, and vegetables. Under the water markets policy, Canal de Bardenas (CB), Canal Imperial (CI), Delta, and Zadorra sell water to other irrigation districts under drought conditions. These water selling districts reduce field crops, while buying districts have higher crop profitability and irrigation efficiency and could maintain fruit trees, vegetables, and even field crops. Investments in efficiency enhancement retain more cropland under production, and when combined with the market policy the water exchanges go down because of lower water scarcity and a more uniform efficiency among districts. The Jalon irrigation district is heavily damaged by drought because water is quite scarce in the left bank of the Ebro, with considerably reductions of field crops for all policy combinations.

Figure 6. Reductions from the baseline scenario of benefits, labor, water diverted, land (field crops, fruit trees, vegetables) in irrigation districts by combinations of market, proportional and efficiency enhancement policies

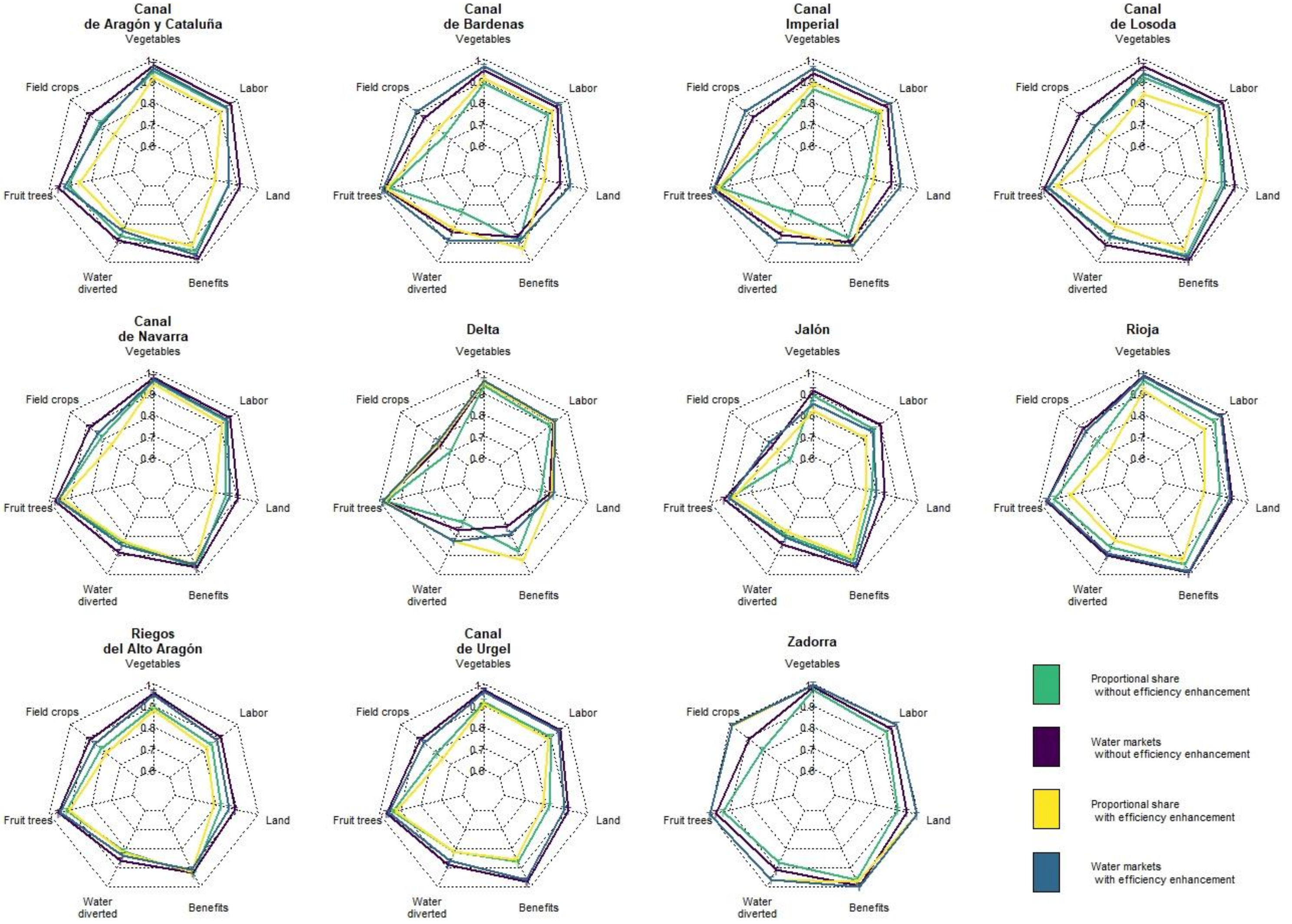

Table 4. Reliability, resilience, vulnerability and sustainability index by climate and policy scenarios.

	Reliability	Resiliency	Vulnerability	Sustainability
Without climate change				
Without efficiency enhancements				
Proportional share	0.76	0.73	0.78	0.43
Water markets	0.78	0.76	0.81	0.48
With efficiency enhancements				
Proportional share	0.85	0.83	0.83	0.58
Water markets	0.86	0.83	0.86	0.62
With climate change				
Without efficiency enhancements				
Proportional share	0.63	0.45	0.77	0.22
Water markets	0.64	0.46	0.80	0.24
With efficiency enhancements				
Proportional share	0.79	0.57	0.82	0.37
Water markets	0.80	0.59	0.85	0.40

Labor reductions depend on crop patterns, with large declines in districts specializing in vegetables and fruit trees that use labor intensively. Labor losses are up to 20% in Jalon and Riegos del Alto Aragon districts. The combination of market and efficiency enhancement policies maintains labor, although losses are important in water selling districts.

Reliability is measured by the proportion of time periods in which baseline cropland water demand is met by the water system, resilience is measured by the recovery duration after the water system fails, and vulnerability is measured by the benefits losses from water system failure (index decreases for more vulnerability). Then, the sustainability index is defined as the product of reliability, resilience and vulnerability (see details in section 2 of the appendix).

The indexes for reliability, resilience, vulnerability and sustainability by policy combination are shown in Table 4. Climate change raises the likelihood of system failure with longer recovery periods and lower benefits. These reduced reliability and resilience and increased vulnerability, make the system less sustainable. The sustainability of the

Figure 7. Joint distribution of drought duration (months) and drought intensity (Mm^3).

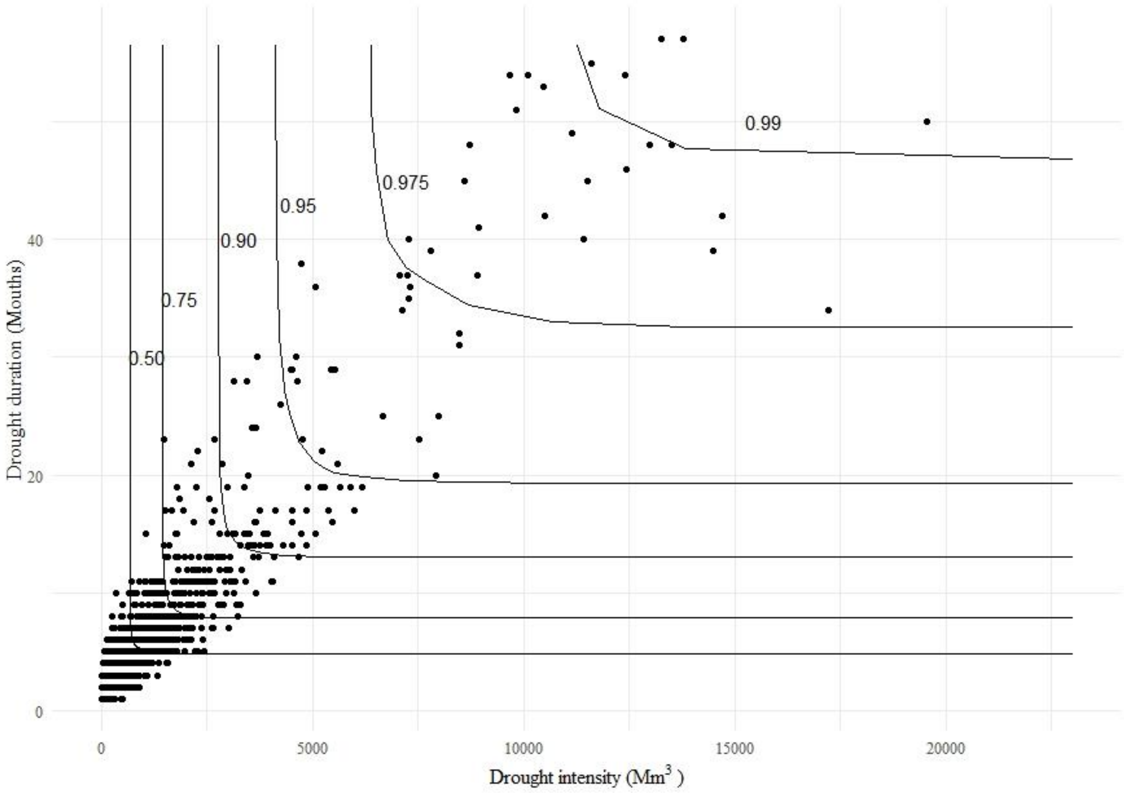

system improves by combining water markets and efficiency enhancements, with gains in reliability, resilience and vulnerability.

Figure 7 shows the joint distribution of drought duration and drought intensity. Drought events are identified by falling basin inflows below a threshold, defined at 75 percent of baseline monthly inflows. The drought period starts when inflows fall below the threshold and finishes when inflows recuperate, with the duration being the number of months under drought. The monthly deficit is the gap between the drought observed inflows and the drought threshold, and drought intensity is the sum of monthly deficits over the drought spell. Around 90 percent of drought spells are shorter than 12 months with water deficit below 2,500 Mm^3. Drought spells longer than two years with water deficits above 5,000 Mm^3 have a 5 percent probability. In extreme cases, the drought duration reaches 60 months with deficits above 20,000 Mm^3.

Figure 8. Conditional exceedance of probability of benefit losses for increasing drought severity.

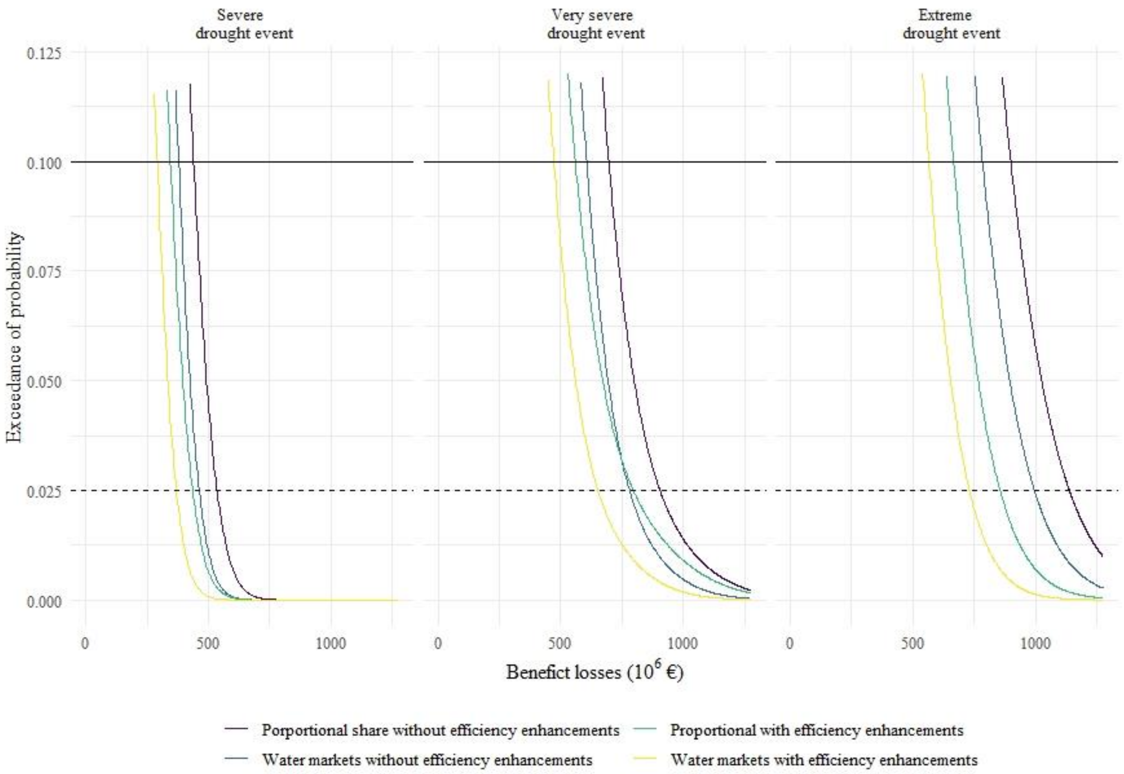

Under a severe drought spell (19 months duration and 4.128 Mm^3 deficit), the probability of accumulated benefit losses exceeding 250 M€, range between 12.5% and 37.5% for the different policy combinations. Combining water markets and efficiency enhancements divides by three the probability that benefit losses exceed 250 M€ under severe drought. The probability than benefit losses exceed 500 M€ is close to 5% in a severe drought spell for proportional share without efficiency enhancements, but the probability decreases below 1.5% for all other policy combinations.

Extreme droughts (47 months and a deficit of 11,146 Mm^3) trigger benefit losses that exceed 500 M€ in half of the cases for the proportional share policy, and 250 M€ with the combination of water markets and efficiency enhancements (Figure A11). For the 5% of worst cases, benefits losses exceed 1,000 M€ under proportional share without efficiency enhancements, and 650 M€ under water markets and efficiency enhancements (Figure 8).

Figure 9 shows how conditional benefit losses depend on the duration and intensity of drought, by policy combination. Benefit losses correspond to quantiles 0.5 (50%) and 0.99 (99%), and contour lines show additional benefit losses of 100 M€. The benefit losses in the first and second columns are for proportional share and water market, without

Figure 9. Contour lines of benefit losses (10^6 €), by policy at quantiles 0.5 and 0.99

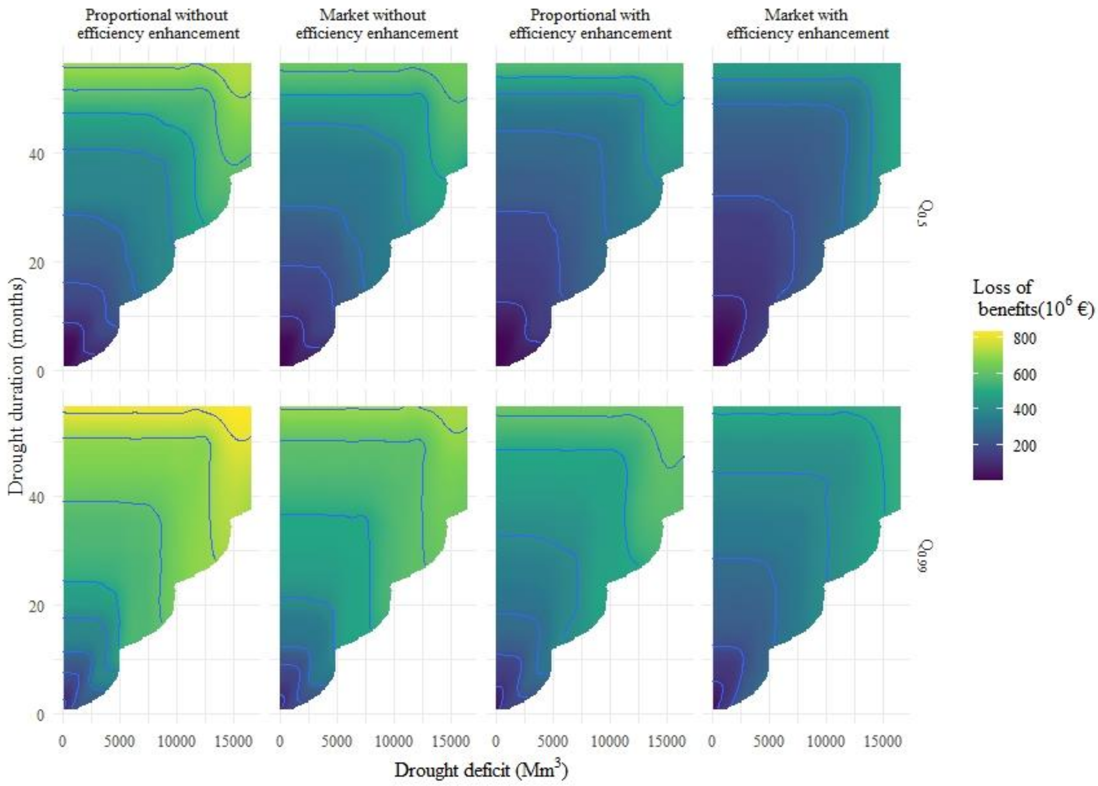

efficiency enhancements, while the third and fourth columns are for combinations with efficiency enhancements. The rows show the conditional quantile benefit losses at 0.5 and 0.99 probabilities.[3]

The combination of water markets and efficiency enhancements reduces benefit losses by almost half (probability 0.5), and by one third in extreme cases (probability 0.99). However, this policy combination also shrinks environmental flows, further degrading water dependent ecosystems.

The more frequent droughts are shorter than 12 months with water deficits under 2,500 Mm^3, and their benefit losses are below 100 M€ with a probability of 50% for all policies. In extreme cases (probability 0.99), the droughts up to 12 months have benefit losses around 300 M€ for proportional share, shrinking to 200 M€ when combining water markets and efficiency enhancements. This indicates that droughts of short duration and low intensity could involve substantial benefit losses, and that the gap in policy performance is greater in adverse cases.

[3] This information is extend to quantiles 0.5, 0.9, 0.95 and 0.99 in figure A12 of the appendix.

Table 5. Percentage of flow gaps between non-complying and minimum environmental flows by policy combination*

	Without climate change	*With climate change*
Without efficiency enhancements		
Proportional share	8.9%	11.9%
Water markets	9.9%	13.7%
With efficiency enhancements		
Proportional share	11.6%	14.6%
Water markets	12.3%	16.2%

* These are the average percentages during drought periods.

For longer and more intense droughts (between 12 and 24 months and between 2,500 and 5000 Mm^3), there is a sharp increase in benefit losses. In extreme cases (probability of 0.99), benefit losses rise to 500 M€ for proportional share, but only to 300 M€ for the combination of water markets and efficiency enhancements. The join probability of having a drought longer than 4 years and with deficits greater than 12,500 Mm^3 is lower than one percent. In these extreme drought events, the combination of water markets and efficiency enhancement reduces benefits losses by 300 M€ compared to proportional share and current irrigation efficiency. The sequence of annual droughts is usually a mix of moderate, severe and extreme drought events, and extreme droughts lasting consecutive years are very rare. For prolonged droughts, the system cannot longer relieve water scarcity because water storage in dams is depleted. Once the dam storage is exhausted, the only response to drought is sharing the remaining water with adjustments in crop patterns.

3.2 Sustainability of the water systems for irrigation and the environment

Ecosystems in the Ebro basin are protected by minimum environmental flows in river reaches across the basin, which are set-up by the Ebro Basin Authority in the basin plan. These environmental flows are minimum levels of stream flows that maintain the status of water-dependent ecosystem. The environmental flows are gauged in 15 river reaches in the basin.

The percentage of the flow gap between non-complying and minimum environmental flows provide information on expected environmental damages. Table 5 shows the average percentage of the flow gap between non-complying and minimum environmental flows during drought periods. The percentages indicate the size of the flow gap for each policy combination, and the ensuing impairment of ecosystems. Efficiency enhancements

Table 6. Sustainability indexes for irrigation, environment and the whole system by climate and policy scenario.

	Irrigation sustainability	Environmental sustainability	Water system sustainability
Without climate change			
Without efficiency enhancements			
Proportional share	0.43	0.91	0.39
Water markets	0.48	0.90	0.43
With efficiency enhancements			
Proportional share	0.58	0.88	0.51
Water markets	0.62	0.87	0.54
With climate change			
Without efficiency enhancements			
Proportional share	0.22	0.88	0.19
Water markets	0.24	0.86	0.21
With efficiency enhancements			
Proportional share	0.37	0.85	0.31
Water markets	0.40	0.83	0.33

and water market policies, together with climate change, aggravate non-compliance, especially the policy of efficiency enhancements that maintains crop production at the expense of ecosystems' degradation.

The environmental sustainability is measured by the average proportion of minimum environmental flows covered by each policy combination during droughts (Table 6). This environmental sustainability index is highest for proportional share water allocation without efficiency enhancements, and lowest for water markets with efficiency enhancements. Water allocation by the current proportional share policy promotes environmental sustainability, while water markets promote irrigation sustainability. However, the differences in environmental sustainability by policy combination are small compared with the differences in irrigation sustainability.

The entire water system sustainability is assessed by multiplying the irrigation sustainability and the environmental sustainability indexes (Table 6). The combination of water markets and efficiency enhancements provide the highest ranking for the water system, and the combination of proportional share without efficiency enhancements the lowest. Decision makers have to decide the policy mix to be chosen by considering the tradeoff between irrigation benefits and environmental protection. The tradeoff indicates that small increases in environmental protection require incurring in large losses in irrigation benefits.

However, the environmental damages can be underestimated for irrigation efficiency investments, as a consequence of the "paradox of irrigation efficiency" (Grafton et al. 2018). The paradox states that higher efficiency rarely reduces water consumption (evapotranspiration) by crops for the same water withdrawals, and the consequence is a fall in irrigation returns that reduce basin stream flows. To confront the paradox, investments in efficiency gains must be coupled with virtuous collective action outcomes capable of preventing the expansion of water consumption by crops.

The result of higher benefits from water markets compared with proportional share, highlighted in this study, is consistent with the findings in the hydroeconomic analysis literature (e.g. Crespo et al., 2019; Escriva-Bou et al., 2017 and Salman et al., 2017). Many studies find that gains in irrigation efficiency reduce the impacts of drought, water scarcity and climate change (Bekchanov et al., 2016; Sánchez-Chóliz and Sarasa, 2019). However, the "paradox of irrigation efficiency" mentioned above will undermine this finding, unless the expansion of water consumption by efficiency gains is prevented. Connor and Kaczan (2013) describe this downside of water markets for in-stream flows in the Murray-Darling basin in Australia, indicating that Australia has chosen trading on water extractions instead of trading in water consumption, in order to reduce the transactions costs of water markets.

Climate change modifies the reliability, resilience and vulnerability of water systems, because of the shift in both water supply and demand (Gau et al. 2019). Despite considerable water management efforts, the sustainability of water systems can be threatened by the conflicting goals of maintaining irrigation and protecting the environment. Folke et al. (2004) recommend a secure range of water allocations for ecosystems, given the uncertainty in ecological responses involving irreversible regime shifts and tipping points.

The present study could be further expanded for a better assessment of the Ebro water system. Possible improvements include modeling the environmental benefits linked to the response of ecosystems to stream flows, and adding the hydropower sector to the economic activities in the basin. Other possible enhancement is to consider the spatial variability of water inflows in stream flows simulations, given the local heterogeneity of climate change impacts across sub-basins.

4. Conclusion

This study analyzes the economic impacts of drought and water scarcity in the Ebro basin, under current and future climate conditions. Climate change projections point toward more frequent, intense and longer drought spells. Reliability, resilience, and vulnerability of the water system to droughts are examined under several water management alternatives. The evaluated policies are the combinations of proportional share or water markets, with current or enhanced irrigation water efficiencies. The assessment of risk provides information on the water system exposure to extreme events, which is important for water management.

Hydroeconomic analysis is conducted with a model that integrates hydrological, economic, and environmental components into a framework that emphasizes the temporal and spatial relationships between water usages. Water inflows are generated using the copula approach, in order to represent both historical stream flows and projected stream flows under weather conditions with longer and more intense droughts. This study is innovative in the assessment of water scarcity impacts, by taking into account that the duration, intensity, and frequency of droughts are changing in the coming decades. The results are examined in terms of probability given the intrinsic uncertainty of drought events and climate change.

Growing crop water requirements, reductions in water inflows, and longer and more intense drought events are expected outcomes from climate change in the Ebro basin. Droughts under historical and climate change conditions entail cutbacks in water extractions, triggering substantial benefit losses in irrigation. Climate change increases the likelihood of longer and more intense droughts and their negative impacts, and impairs the resilience of the water system exposed to longer recovery periods. The frequency of extreme weather conditions will be also higher, boosting the risk of severe benefit losses. The climate stress will reduce the reliability of the water system to meet both human water security and environmental flows.

The impacts of droughts and climate change can be reduced by combining water markets with investments in irrigation efficiency. This policy mix expands cropland in production, water extractions and irrigation benefits, while lowering their dispersion and uncertainty. The impacts of extreme droughts are reduced somewhat, although the policy effectiveness decreases when droughts are more intense. The combination of water markets and efficiency enhancements improves the system sustainability because vulnerability is reduced, and reliability and resilience are reinforced. However, the gains in efficiency increase water consumption, reducing the basin in-stream flows. Consequently, this policy hinders the compliance with environmental flows and jeopardizes the status of aquatic ecosystem. Therefore, irrigation benefits are maintained at the expense of the environment.

The duration of most droughts is less than one year, and the likelihood of longer droughts shrinks because the probability of consecutive years of drought declines with duration. However, ten percent of droughts are longer than one year, and the ensuing benefit losses over several years can be important. The capacity of the water system to avoid cutbacks during droughts depends on the water storage available in dams. Once the capability of dams to offset water scarcity is exceeded, the reactions to droughts are limited to adjustments in crop patters and water trading. Water markets and efficiency enhancements are good interventions to maintain irrigation activities, at the cost of degrading aquatic ecosystems, and the trade-off has to be settled by decision makers.

Acknowledgements

This study has been financed by the projects INIA RTA2014-00050-00-00 and INIA RTA2017-00082-00-00 of the Ministry for Science and Innovation, partly financed by European ERDF funds, and by support received from the ECONATURA research group of the Government of Aragon. Daniel Crespo has conducted this study with the support of a PhD grant from INIA. Part of the work by Daniel Crespo was developed at the Water Program of the International Institute for Applied Systems Analysis (IIASA). Special assistance has been provided by María Ángeles Lorenzo and Daniel Isidoro (CITA-DGA), and by Rogelio Galván and Miguel Ángel García Vera (CHE-MITECO).

References

Arbués, F., Barberán, R., Villanúa, I., 2004. Price impact on urban residential water demand: A dynamic panel data approach. Water Resources Research 40. https://doi.org/10.1029/2004WR003092

Bekchanov, M., Ringler, C., Bhaduri, A., Jeuland, M., 2016. Optimizing irrigation efficiency improvements in the Aral Sea Basin. Water Resources and Economics 13, 30–45. https://doi.org/10.1016/j.wre.2015.08.003

Borgomeo, E., Pflug, G., Hall, J.W., Hochrainer-Stigler, S., 2015. Assessing water resource system vulnerability to unprecedented hydrological drought using copulas to characterize drought duration and deficit. Water Resour. Res. 51, 8927–8948. https://doi.org/10.1002/2015WR017324

Brown, C.M., Lund, J.R., Cai, X., Reed, P.M., Zagona, E.A., Ostfeld, A., Hall, J., Characklis, G.W., Yu, W., Brekke, L., 2015. The future of water resources systems analysis: Toward a scientific framework for sustainable water management. Water Resour. Res. 51, 6110–6124. https://doi.org/10.1002/2015WR017114

Brunner, M.I., Slater, L., Tallaksen, L.M., Clark, M., 2021. Challenges in modeling and predicting floods and droughts: A review. WIREs Water 8. https://doi.org/10.1002/wat2.1520

Büntgen, U., Urban, O., Krusic, P.J., Rybníček, M., Kolář, T., Kyncl, T., Ač, A., Koňasová, E., Čáslavský, J., Esper, J., Wagner, S., Saurer, M., Tegel, W., Dobrovolný, P., Cherubini, P., Reinig, F., Trnka, M., 2021. Recent European drought extremes beyond Common Era background variability. Nature Geoscience 14, 190–196. https://doi.org/10.1038/s41561-021-00698-0

Cammalleri, C., Naumann, G., Mentaschi, L., Formetta, G., Forzieri, G., Gosling, S., Bisselink, B., De Roo, A., Feyen, L., Commission, E., Centre, J.R., 2020. Global warming and drought impacts in the EU : JRC PESETA IV project : Task 7. Publications Office. https://doi.org/doi/10.2760/597045

Chen, L., Singh, V.P., Guo, S., Zhou, J., Zhang, J., 2015. Copula-based method for multisite monthly and daily streamflow simulation. Journal of Hydrology 528, 369–384. https://doi.org/10.1016/j.jhydrol.2015.05.018

Connor, J.D., Kaczan, D., 2013. Principles for Economically Efficient and Environmentally Sustainable Water Markets: The Australian Experience, in: Schwabe, K., Albiac, J., Connor, J.D., Hassan, R.M., Meza González, L. (Eds.), Drought in Arid and Semi-Arid Regions. Springer Netherlands, Dordrecht, pp. 357–374. https://doi.org/10.1007/978-94-007-6636-5_20

Crespo, D., Albiac, J., Kahil, T., Esteban, E., Baccour, S., 2019. Tradeoffs between Water Uses and Environmental Flows: A Hydroeconomic Analysis in the Ebro Basin. Water Resour Manage 33, 2301–2317. https://doi.org/10.1007/s11269-019-02254-3

Escriva-Bou, A., Pulido-Velazquez, M., Pulido-Velazquez, D., 2017. Economic Value of Climate Change Adaptation Strategies for Water Management in Spain's Jucar Basin. Journal of Water Resources Planning and Management 143, 04017005. https://doi.org/10.1061/(ASCE)WR.1943-5452.0000735

Falloon, P., Betts, R., 2010. Climate impacts on European agriculture and water management in the context of adaptation and mitigation—The importance of an integrated approach. Science of The Total Environment 408, 5667–5687. https://doi.org/10.1016/j.scitotenv.2009.05.002

Feyen, L., Gosling, S., Ciscar, J., Ibarreta, D., Commission, E., Centre, J.R., 2020. Climate change impacts and adaptation in Europe : JRC PESETA IV final report. Publications Office. https://doi.org/doi/10.2760/171121

Folke, C., Carpenter, S., Walker, B., Scheffer, M., Elmqvist, T., Gunderson, L., Holling, C.S., 2004. Regime Shifts, Resilience, and Biodiversity in Ecosystem Management. Annual Review of Ecology, Evolution, and Systematics 35, 557–581. https://doi.org/10.1146/annurev.ecolsys.35.021103.105711

García-Ruiz, J.M., López-Moreno, J.I., Vicente-Serrano, S.M., Lasanta–Martínez, T., Beguería, S., 2011. Mediterranean water resources in a global change scenario. Earth-Science Reviews 105, 121–139. https://doi.org/10.1016/j.earscirev.2011.01.006

Generalitat de Cataluya (GC), 2009. Superfícies Municipals Dels Conreus Agrícoles. Any 2009. Departament d'Agricultura, Ramaderia, Pesca, Alimentació i Medi Natural, Barcelona.

Gobierno de Aragón (DGA), 2009. Base de datos 1T de superficies de cultivos por término municipal para El Gobierno de Aragón 2009. Departamento de Desarrollo Rural y Sostenibilidad, Zaragoza.

Gobierno de Navarra (GN), 2009. Base de datos 1T de superficies de cultivos por término municipal para el Gobierno de Navarra 2009. Departamento de Desarrollo Rural, Medio Ambiente y Administración Local.

Grafton, R.Q., Williams, J., Perry, C.J., Molle, F., Ringler, C., Steduto, P., Udall, B., Wheeler, S.A., Wang, Y., Garrick, D., Allen, R.G., 2018. The paradox of irrigation efficiency. Science 361, 748–750. https://doi.org/10.1126/science.aat9314

Guo, Y., Huang, S., Huang, Q., Wang, H., Wang, L., Fang, W., 2019. Copulas-based bivariate socioeconomic drought dynamic risk assessment in a changing environment. Journal of Hydrology 575, 1052–1064. https://doi.org/10.1016/j.jhydrol.2019.06.010

Hashimoto, T., Stedinger, J.R., Loucks, D.P., 1982. Reliability, resiliency, and vulnerability criteria for water resource system performance evaluation. Water Resour. Res. 18, 14–20. https://doi.org/10.1029/WR018i001p00014

Herman, J.D., Quinn, J.D., Steinschneider, S., Giuliani, M., Fletcher, S., 2020. Climate Adaptation as a Control Problem: Review and Perspectives on Dynamic Water Resources Planning Under Uncertainty. Water Resources Research 56, e24389. https://doi.org/10.1029/2019WR025502

Hernández, N., Gil, M., Garrido, A., Rodríguez, R., 2013. La sequía 2005-2008 en al cuenca del Ebro: Vulnerabilidad, impactos y medidas de gestión. UPM-CEIGRAM, Madrid.

Iglesias, A., Garrote, L., Flores, F., Moneo, M., 2007. Challenges to Manage the Risk of Water Scarcity and Climate Change in the Mediterranean. Water Resources Management 21, 775–788. https://doi.org/10.1007/s11269-006-9111-6

Instituto Nacional de Estadística (INE), 2009. Censo Agrario 2009. INE, Madrid.

IPCC, I.P. on C.C., 2014. Climate Change 2014 – Impacts, Adaptation and Vulnerability: Part B: Regional Aspects: Working Group II Contribution to the IPCC Fifth Assessment Report. Cambridge University Press. https://doi.org/10.1017/CBO9781107415386

Kirby, J.M., Connor, J., Ahmad, M.D., Gao, L., Mainuddin, M., 2014. Climate change and environmental water reallocation in the Murray–Darling Basin: Impacts on flows, diversions and economic returns to irrigation. Journal of Hydrology 518, 120–129. https://doi.org/10.1016/j.jhydrol.2014.01.024

Li, Q., Lin, J., Racine, J.S., 2013. Optimal Bandwidth Selection for Nonparametric Conditional Distribution and Quantile Functions. Journal of Business & Economic Statistics 31, 57–65. https://doi.org/10.1080/07350015.2012.738955

Li, Q., Racine, J.S., 2008. Nonparametric Estimation of Conditional CDF and Quantile Functions With Mixed Categorical and Continuous Data. Journal of Business & Economic Statistics 26, 423–434. https://doi.org/10.1198/073500107000000250

Li, Y., Ye, W., Wang, M., Yan, X., 2009. Climate change and drought: a risk assessment of crop-yield impacts. Clim. Res. 39, 31–46. https://doi.org/10.3354/cr00797

Ministerio de Agricultura y Medio Ambiente (MAGRAMA), 2015. Anuario de Estadísticas Agrarias. Ministerio de Agricultura y Medio Ambiente (MAGRAMA), Madrid.

Ministerio de Medio Ambiente y Medio Rural y Marino (MARM), 2010. Valoración de los activos naturales de España. Ministerio de Medio Ambiente y Medio Rural y Marino, Centro de Publicaciones, Madrid.

Mishra, A.K., Singh, V.P., 2011. Drought modeling – A review. Journal of Hydrology 403, 157–175. https://doi.org/10.1016/j.jhydrol.2011.03.049

Naumann, G., Spinoni, J., Vogt, J.V., Barbosa, P., 2015. Assessment of drought damages and their uncertainties in Europe. Environmental Research Letters 10, 124013. https://doi.org/10.1088/1748-9326/10/12/124013

NOAA, 2021. U.S. Billion-Dollar Weather and Climate Disasters. National Centers for Environmental Information, Asheville.

Quiroga, S., Garrote, L., Iglesias, A., Fernández-Haddad, Z., Schlickenrieder, J., de Lama, B., Mosso, C., Sánchez-Arcilla, A., 2011. The economic value of drought information for water management under climate change: a case study in the Ebro basin. Natural Hazards and Earth System Science 11, 643–657. https://doi.org/10.5194/nhess-11-643-2011

Rocheta, E., Sugiyanto, M., Johnson, F., Evans, J., Sharma, A., 2014. How well do general circulation models represent low-frequency rainfall variability?: GCM LOW-FREQUENCY RAINFALL VARIABILITY. Water Resour. Res. 50, 2108–2123. https://doi.org/10.1002/2012WR013085

Salman, D., Amer, S.A., Ward, F.A., 2017. Protecting food security when facing uncertain climate: Opportunities for Afghan communities. Journal of Hydrology 554, 200–215. https://doi.org/10.1016/j.jhydrol.2017.09.015

Salvadori, G., De Michele, C., 2004. Frequency analysis via copulas: Theoretical aspects and applications to hydrological events. Water Resour. Res. 40. https://doi.org/10.1029/2004WR003133

Sánchez Chóliz, J., Sarasa, C., 2019. Uncertainty in Irrigation Technology: Insights from a CGE Approach. Water 11, 617. https://doi.org/10.3390/w11030617

Sandoval-Solis, S., McKinney, D.C., Loucks, D.P., 2011. Sustainability Index for Water Resources Planning and Management. J. Water Resour. Plann. Manage. 137, 381–390. https://doi.org/10.1061/(ASCE)WR.1943-5452.0000134

Spinoni, J., Naumann, G., Vogt, J.V., Barbosa, P., 2015. The biggest drought events in Europe from 1950 to 2012. Journal of Hydrology: Regional Studies 3, 509–524. https://doi.org/10.1016/j.ejrh.2015.01.001

Vicente-Serrano, S.M., Lopez-Moreno, J.-I., Beguería, S., Lorenzo-Lacruz, J., Sanchez-Lorenzo, A., García-Ruiz, J.M., Azorin-Molina, C., Morán-Tejeda, E., Revuelto, J., Trigo, R., Coelho, F., Espejo, F., 2014. Evidence of increasing drought severity caused by temperature rise in southern Europe. Environ. Res. Lett. 9, 044001. https://doi.org/10.1088/1748-9326/9/4/044001

Ward, F.A., 2021. Hydroeconomic Analysis to Guide Climate Adaptation Plans. Front. Water 3, 681475. https://doi.org/10.3389/frwa.2021.681475

Appendix

1. Beta regression for modelling proportions and bounded data

The performance of each policy alternative under different climate conditions is analyzed, by regression, comparing the percentage of cropland reductions over the baseline. OLS estimation is the simplest method, but is not appropriate since the irrigation area and the percentage of cropland reductions are bounded variables.

Sinusoidal regression or logit regression analyze bounded data, like rates and proportions, but they are difficult to interpret and do not treat heteroskedastic problems. In addition, the distribution of proportions could be asymmetric and Gaussian approximations are not appropriate. Beta regression overcome these difficulties assuming that the response variable is beta distributed.

Following the model proposed by Ferrari and Cribari-Nato (2004), the response variable is Beta distributed, $y \sim \mathcal{B}(\mu, \phi)$, and its density function $f(y; \mu, \phi)$ is defined by two parameters μ and ϕ, and takes the expression:

$$f(y; \mu, \phi) = \frac{\Gamma(\phi)}{\Gamma(\mu\phi)\Gamma\big((1-\mu)\phi\big)} y^{\mu\phi-1}(1-y)^{(1-\mu)\theta-1}, \qquad 0 < \mathrm{y} < 1$$

where μ and ϕ are the precision and dispersion parameters, respectively, and satisfy that $0 < \mu < 1$ and $\phi > 0$. The mean and variance of the beta distribution are expressed with the precision and dispersion parameters as:

$$E(y) = \mu \text{ and } VAR(y) = \mu(1-\mu)/(1+\phi)$$

As in generalized linear models (GLM), the precision parameter is linked to the covariates, x, by a link function, $g_1(\mu)$, and a linear predictor, $x'\beta_\mu$; and the dispersion parameter is linked to another set of covariates, z, by a second link function, $g_2(\phi)$, and a linear predictor, $z'\beta_\phi$.

$$g_1(\mu) = x'\beta_\mu$$
$$g_2(\phi) = z'\beta_\phi$$

The coefficient sets β_μ and β_ϕ are estimated by Maximum Likelihood (ML). The logit, probit or loglog are functions commonly used as link functions. A comprehensive explanation of the model can be found at Cribari-Neto and Zeileis (2010).

The assumptions in the model are:

1) The percentage of cropland reductions over the baseline is beta distributed.

2) The precision and dispersion parameters are fitted by the percentage of the annual inflows over the baseline inflows, year, climate change and policy combination.

3) The logit link function and log link function connect the precision parameter and dispersion parameter, respectively, with the covariate sets.

The logit link function has been selected because the coefficients estimated indicate odds ratios, and the log link function ensures that dispersion parameter is greater than zero. Table A1 in the appendix shows the results of the estimation. The percentage crop reduction under different drought intensity, climate change, year, and policy showed in table 2 are computed with the results of the beta regression.

Table A1. Beta regression estimation results (standard deviation in brackets)

	Dependent variable:	
	Percentage of cropland reductions over the baseline	
	M.1	M.2
Precision (μ) model with logit link		
Year	0.023***	0.023***
	(0.001)	(0.001)
Proportional share	0.226***	0.221***
	(0.019)	(0.016)
Climate Change	0.081***	0.081**
	(0.028)	(0.028)
Enhancement of efficiency	-0.787***	-0.787***
	(0.019)	(0.019)
Inflows	-4.232***	-4.230***
	(0.035)	(0.035)
Intercept	-0.516***	-0.513***
	(0.040)	(0.040)
Dispersion (ϕ) model with log link		
Year	0.010***	0.008***
	(0.001)	(0.001)
Proportional share	-0.018	
	(0.030)	
Climate Change	0.470***	0.470***
	(0.040)	(0.040)
Enhancement of efficiency	0.277***	0.277***
	(0.030)	(0.030)
Inflows	2.314***	2.310***
	(0.053)	(0.053)
Intercept	0.817***	0.809***
	(0.058)	(0.056)
Observations	9,020	9,020
R^2	0.650	0.650
Log Likelihood	15,536	15,535
Note:		***p<0.001; **p<0.01

2. Reliability, resilience, vulnerability and sustainability index

Water management seeks to maintain the water system in a satisfactory state. The threshold for determining system failure is settled as the 75 percent of the baseline cropland water demand, and therefore the water system is in a satisfactory state if the 75 percent of the water demand at the baseline is meet. Reliability (Rel) measures the capacity of the water system to maintain a satisfactory state, and it is the number of the years over the total number of years (n) in which water system operates satisfactorily (S_i). In terms of probability, reliability is the probability of the water system to satisfy the 75 percent of the irrigation water demand.

$$S_i = \begin{cases} S_i = 1\ if\ Div > \ 0.75 * Div_{baseline} \\ S_i = 0\ if\ Div < 0.75\ * Div_{baseline} \end{cases} \qquad Rel = \frac{\sum S_i}{n} = P(S_i = 1)$$

System resilience (Res) measures the recovery capacity of the system after a system failure. Then, resilience is the frequency with which the system recovers from failure

$$Res = P(S_{i+1} = 1 \mid S_i = 0) = \frac{P(S_i\ = 0\ \cap S_{i+1}\ = 1)}{P(S_i = 0)}$$

Vulnerability (Vul) of the water system is measured by the benefit losses in the water system. Vulnerability is defined by the mean value of irrigation benefits (π_i) over irrigation benefits in the baseline ($\pi_{baseline}$), when the system is in an unsatisfactory state:

$$Vul = \frac{1}{\sum_i^n (1 - S_i)} \cdot \sum_i^n (1 - S_i) \cdot \frac{\Pi_i}{\pi_{baseline}}$$

Sustainability Sus is measured as the product of the reliability, resilience and vulnerability

$$Sus = Rel * Res * Vul$$

3. Probably, exceedance of probability and conditional probability

Probability is an important concept in this study that is used in several indicators used in the analysis of the results. In order to clarify concepts as exceedance of probability or Value at Risk, the concept of probability is briefly explained. Probability is a measure of the likelihood of an event happening. For a continuous random variable X, the probability that X takes a value lower than x is expressed as $P(X \leq x)$; and the probability that the variable exceeds a certain value is named exceedance of probability, that is $P(X > x) = 1 - P(X \leq x)$.

The cumulative distribution function (c.d.f.) $F_X(x)$ is defined as $F_x(x) = P(X \leq x)$; and the complementary cumulative distribution function (c.c.d.f.) (tail distribution or exceedance of probability function) is a function that account the probability that X is equal or greater than x, and it is expressed as:

$$\widetilde{F_X}(x) = P(X > x) = P(X \geq x) = 1 - P(X \leq x) = 1 - F_X(x)$$

The inverse function of c.d.f. is the quantile function $q(\alpha)$, and is the minimum value of the amongst x that the c.d.f. excess the value α:

$$q(\alpha) = F_X^{-1}(x) = \inf\{x \mid F_X(x) = P(X \leq x) \geq \alpha\}$$

Value at Risk (VaR) is a risk metric that indicates the maximum benefit losses given a probability level, and is obtain with the quantile function. Benefits losses can be accounted with a positive value or with a negative value. In case that benefit losses X are expressed as a negative value, $X < 0$, the VaR is the lower α- quantile of the random variable X and is defined as

$$VaR_\alpha(x) = \inf\{ x \mid P(X \leq x = VaR) \geq \alpha\}$$

and when benefit losses are greater than zero, $X > 0$, the VaR is obtained by the exceedance of probability:

$$VaR_\alpha(x) = \inf\{ x \mid P(X \geq x = VaR) \geq 1 - \alpha\}$$

VaR provides information about uncertainty and risk, and it is appropriate to compare water management alternatives.

The economic impact of a drought spell is the accumulated annual benefit losses in relation to the baseline throughout the episode, and depends on its duration and intensity. The conditional probability of benefit losses given certain duration and intensity of a drought spell indicates the exposure of the system to that drought event, since it measures the probability of an event given the occurrence of another events. The conditional probability of the random variable Y given X_1 and X_2 is expressed as

$$F_{Y|X=x}(y) = P(Y \leq y \mid X_1 = x_1, X_2 = x_2)$$

and the conditional quantile is given by the expression

$$F^{-1}_{Y|X=x}(\alpha) = \inf\{y \in \mathbb{R} \,|F_{Y|X=x}(y) \geq \alpha\}$$

Its definition is straightforward from quantile definition: the minimum value of y from amongst all those values of whose c.d.f. value excess the value α given the events $X_1 = x_1$ and $X_2 = x_2$. A different way to express the conditional quantile function is

$$F_{Y|X=x}(y) = P(Y \leq y \,|X_1 = x_1, X_2 = x_2) = \alpha$$

The maximum benefit losses at a certain level of probability α given a drought duration and a drought intensity is obtain from the quantile that satisfices

$$P(L \leq l |\, D = d, I = i) = \alpha$$

where L is benefit losses in M€, D is drought duration in months and I is drought intensity in Mm^3. The VaR of irrigation benefits given a drought spell with certain duration and intensity is obtain from the conditional probability and the conditional quantile.

Non-parametric estimators and copulas approach estimate the conditional probability and the quantile required to compute the VaR. Non parametric estimators are computationally demanding and copula approach could be preferred when the number of estimations is large. The non-parametric method proposed by Li et al. (2013) estimates the conditional quantile function $q_\alpha(x_1, \dots, x_n)$ by numerically inverting the estimated conditional distribution function $\hat{F}(y|x_1, \dots, x_n)$ and solving:

$$\hat{q}_\alpha(x_1, \dots, x_n) = \underset{x}{\operatorname{argmin}} \,|\alpha - \hat{F}(q|x_1, \dots, x_n)|$$

The conditional distribution function and the conditional quantile function are estimated in R with the package np developed by Hayfield and Racine (2008). The exceedance of probability at figure 8 and figure A11 are estimated by the non-parametric method.

The conditional quantile based on copulas is an alternative method to non-parametric (Kraus and Czado, 2016). The joint distribution $F(x_1, x_2, x_3)$ of a multivariate random vector is expressed in terms of a copula $C\big(F(x_1), F(x_2), F(x_3)\big)$. Then, the density function $f(x_1, x_2, x_3)$ can be expressed as

Table A2. Copula and parameters of the join function of benefits losses (L), drought duration (D) and drought intensity (I).

Scenario	Copula	Type	θ_1	θ_2	τ
Without efficiency enhancements					
Proportional share					
	C_{ID}	Gumbel	3.62	-	0.72
	C_{LD}	Survival Clayton	2.37	-	0.54
	$C_{LI\|D}$	BB8	1.42	0.99	0.18
Water markets					
	C_{ID}	Gumbel	3.62	-	0.72
	C_{LD}	Survival Clayton	2.37	-	0.54
	$C_{LI\|D}$	BB8	1.40	0.99	0.18
With efficiency enhancements					
Proportional share					
	C_{ID}	Gumbel	3.62	-	0.72
	C_{LD}	Survival Clayton	2.09	-	0.72
	$C_{LI\|D}$	BB8	1.43	0.99	0.19
Water markets					
	C_{ID}	Gumbel	3.62	-	0.72
	C_{LD}	Survival Clayton	2.04	-	0.51
	$C_{LI\|D}$	BB8	1.41	1.00	0.18

$$f(x_1, x_2, x_3) = f_1(x_1) \cdot f_2(x_2) \cdot f_3(x_3) \cdot c_{12}\{F_1(x_1), F_2(x_2)\} \cdot c_{23}\{F_2(x_2), F_3(x_3)\} \cdot c_{13|2}\{F(x_1|x_2), F(x_3|x_2)\}$$

where $c(\cdot,\cdot)$ is the copula density (Aas et al., 2009) and the estimation of the conditional quantile function is obtained following Kraus and Czado (2016).

The conditional quantile in figure 9 and figure A12 is estimated by the copula method, since the non-parametric approach is impracticable due to the number of estimations needed for the grid. The join function distribution of benefit losses, drought duration and drought intensity is estimated with a C-Vine copula that combine bivariate copulas. Tabla A2 shows the structure of the C-Vine and parameter estimations.

4. The join probability of drought duration and drought intensity

Gumbel copula describes asymmetry dependence and it is used to capture strong upper tail dependence and weak lower tail dependence. The joint distribution of drought duration and drought intensity is obtained from a Gumbel Copula and it takes the form:

$$C(u, v) = \exp\left[-\left((-\ln(u))^{\theta} + (-\ln(v))^{\theta}\right)^{\frac{1}{\theta}}\right]$$

The marginal distributions of the copula are the empirical distributions and the parameter of the copula is estimated by maximum likelihood.

5. Figures

Figure A1. Boxplot of the mean (left) and standard deviation (right) of 1.000 realizations of monthly streamflow generated with copula parameter θ

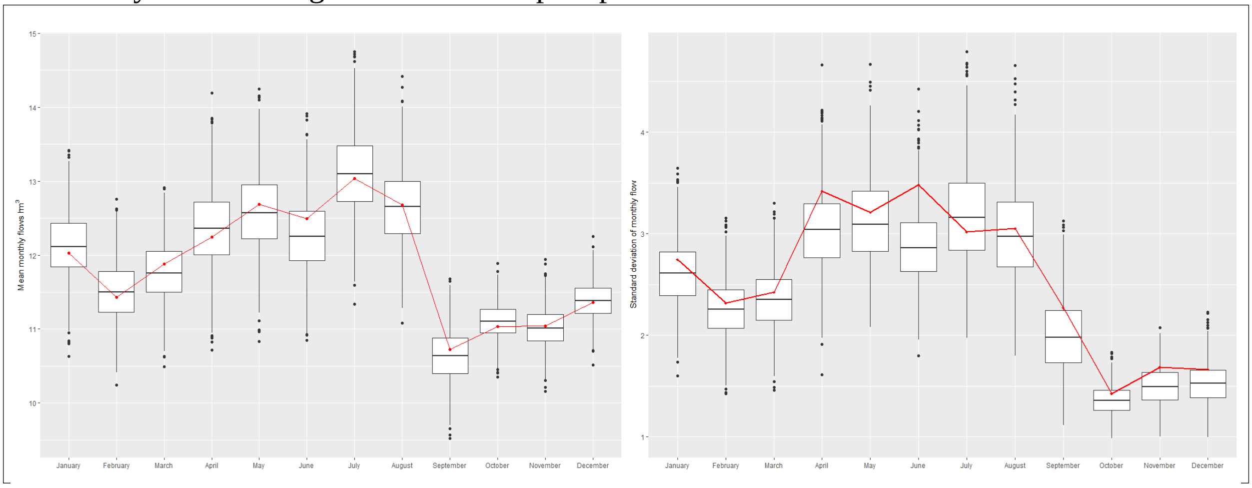

Figure A2. Boxplot of the mean (left) and standard deviation (right) of 1.000 realizations of monthly streamflow generated with copula parameter 2θ

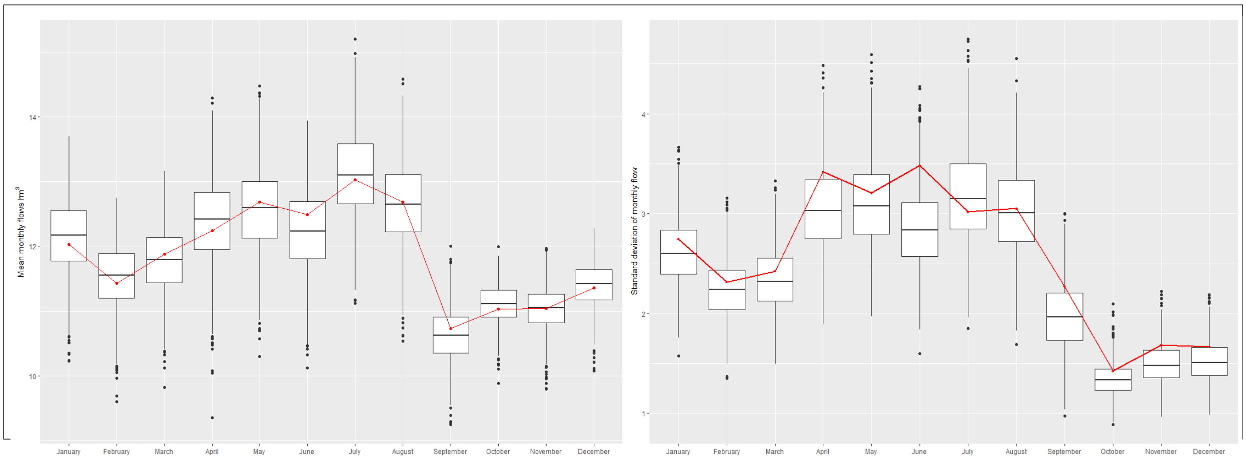

Figure A3. Boxplot of the autorrelation function of 1.000 realizations of monthly streamflow generated with copula parameter θ (left) and 2θ

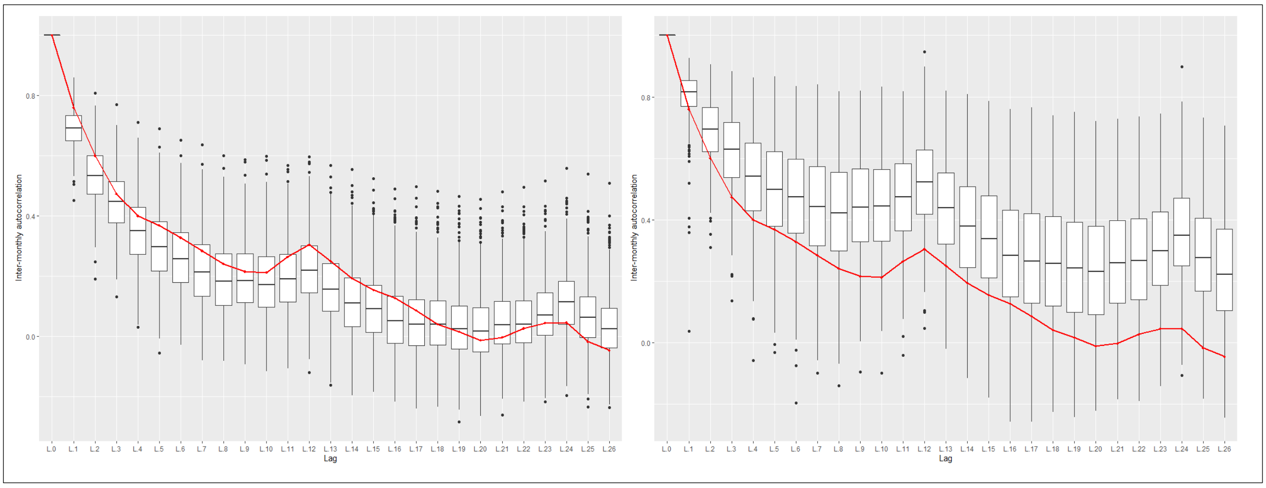

Figure A4. Estimated marginal means of cropland reduction over the baseline scenario by policy and climate change scenario. Confidence interval at 95%.

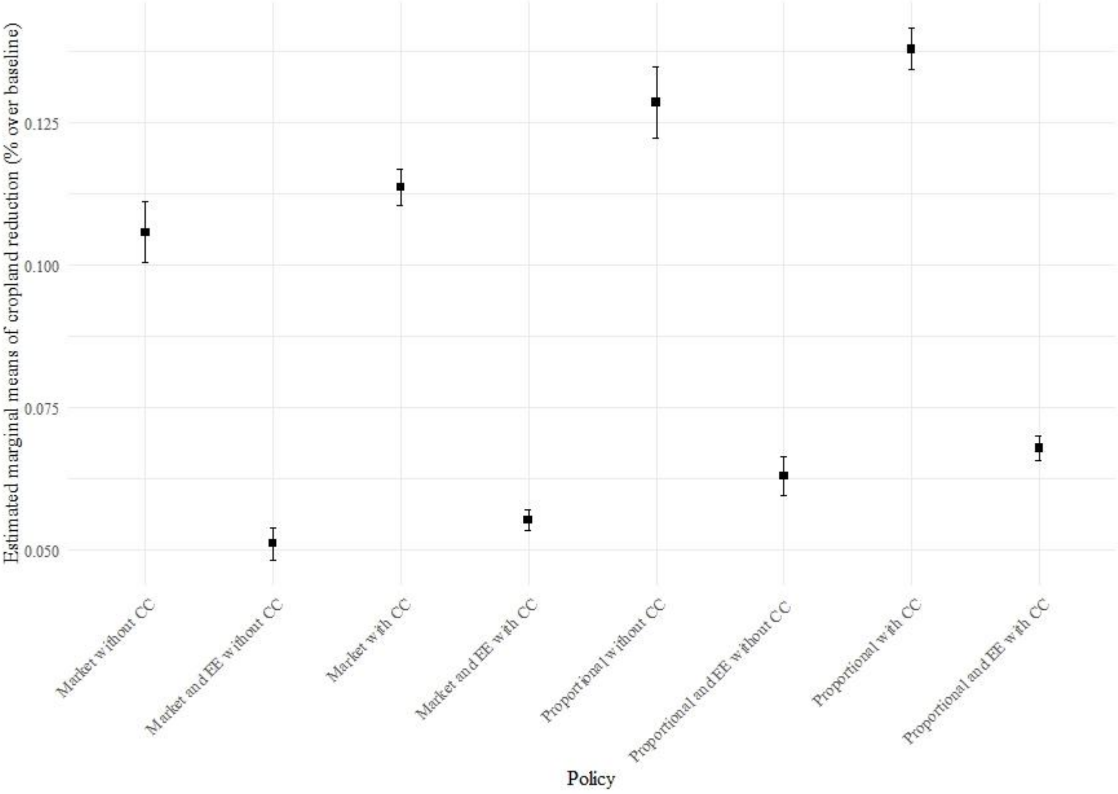

EE means Enhance of efficiency and CC is climate change

Figure A5. Cropland distribution under irrigation land reduction

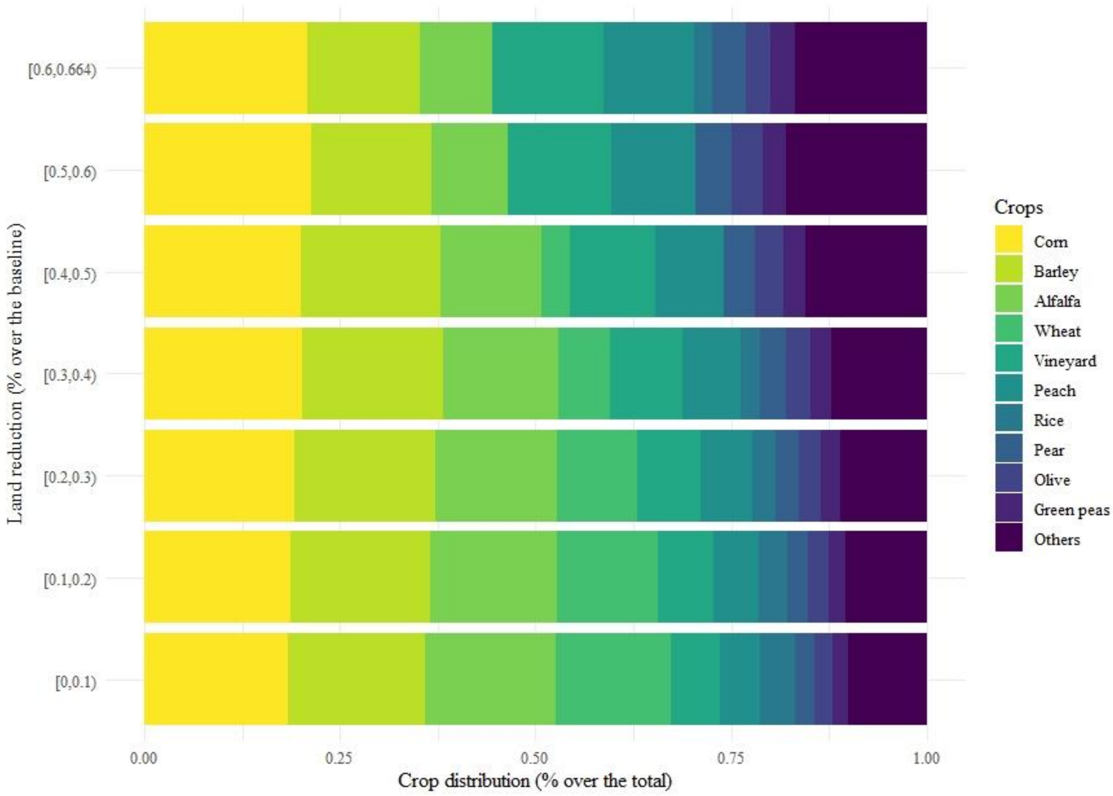

Figure A6. Concentration index under policy scenario

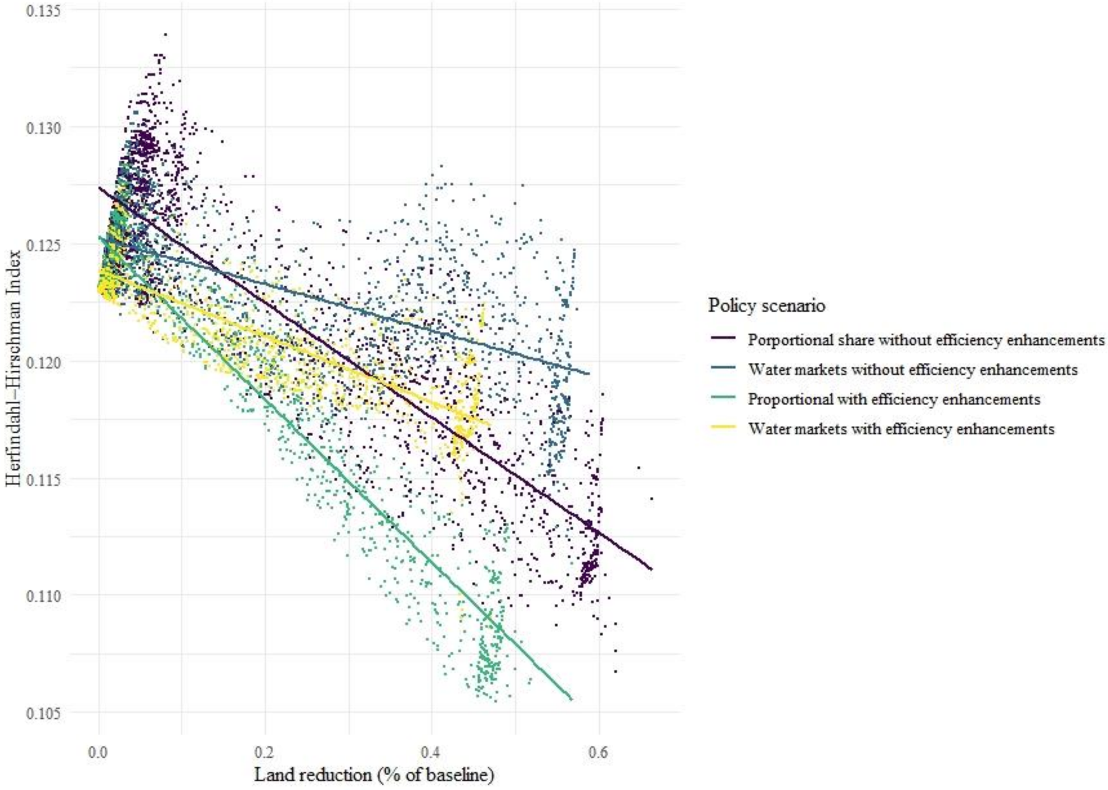

The figure A6 shows the Herfindahl-Hirschman concentration index under policy scenario and it is defined as:

$$H = \sum_{i=1}^{N} s_i^2$$

where s_i is the share of the crop i over the total land and N is the number of crops. The index measures the production concentration, specialization, and sharing. Higher values of H means higher concentration.

Figure A7. Monthly water deficit (Mm^3) and water scarcity index

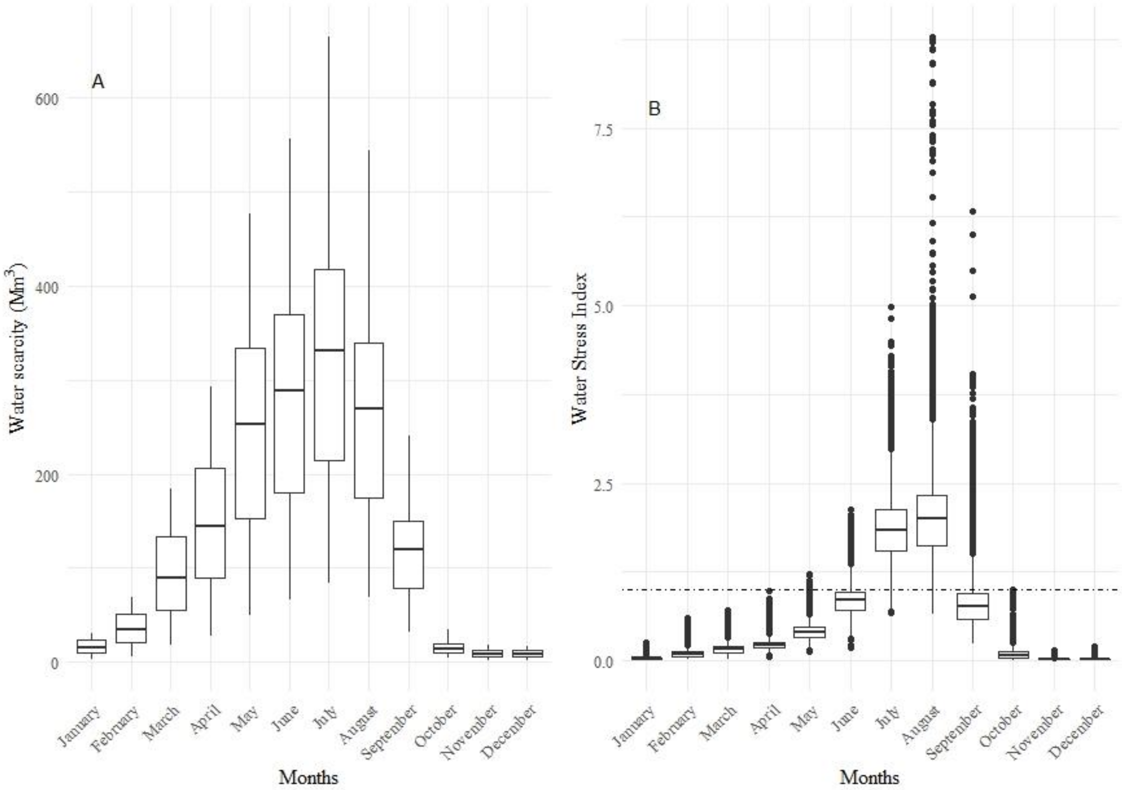

Figure A8. Comparison of water use by policy with and without efficiency enhancements under the same climate conditions

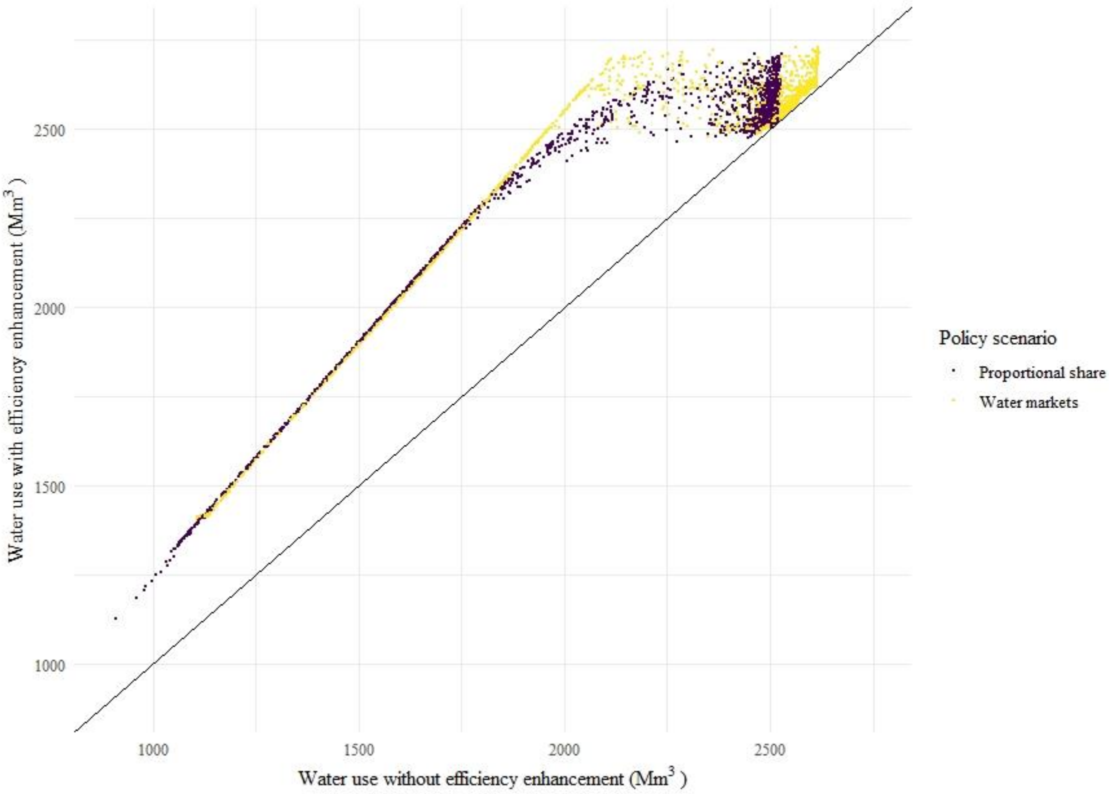

Figure A9. Distribution of the fall in streamflow at the river mouth from investments in efficiency enhancements (Mm^3)

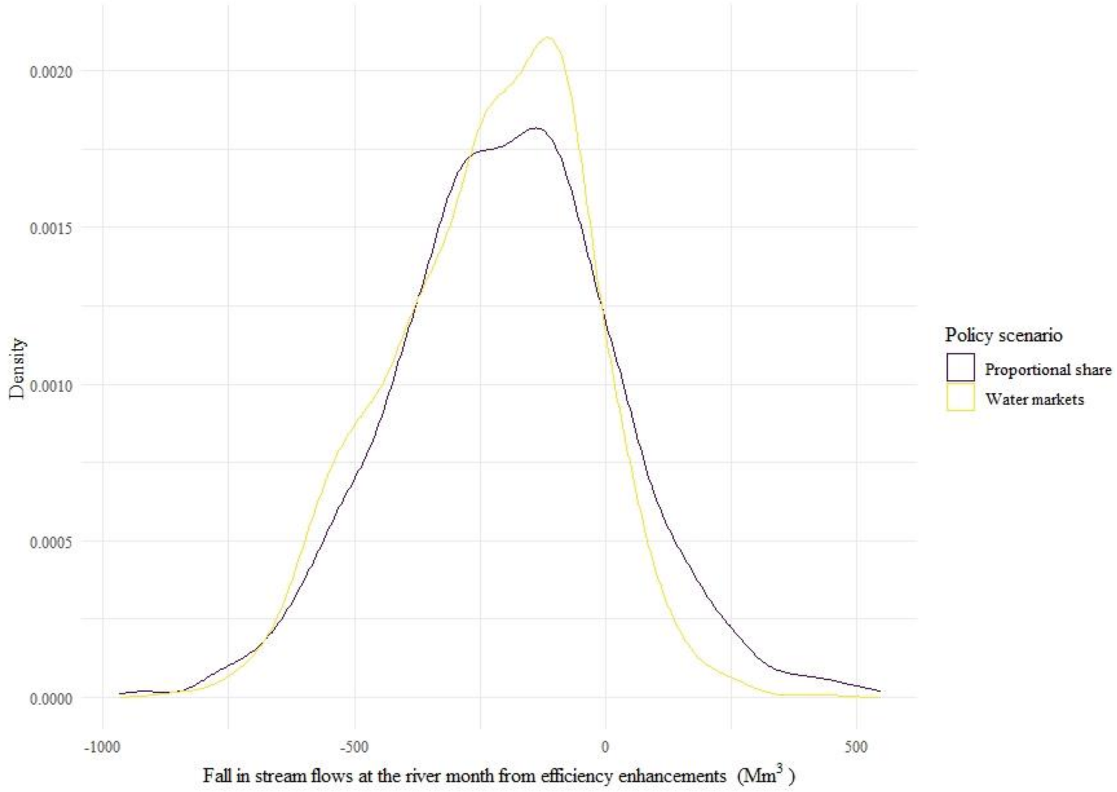

Figure A10. Probability of annual benefits and exceedance of probability of annual benefit losses (10^6 €)

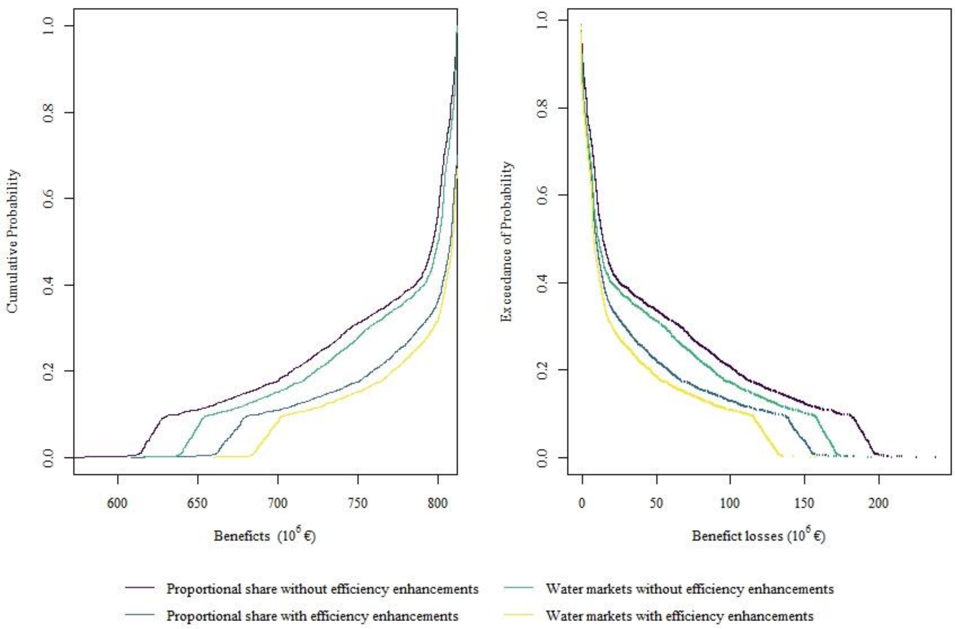

Figure A10 shows the cumulative probability of the annual irrigation benefits and the exceedance of probability of losses under market and proportional policies with and without efficiency enhancement.

Figure A11. Conditional exceedance of probability of benefit losses under different drought spells.

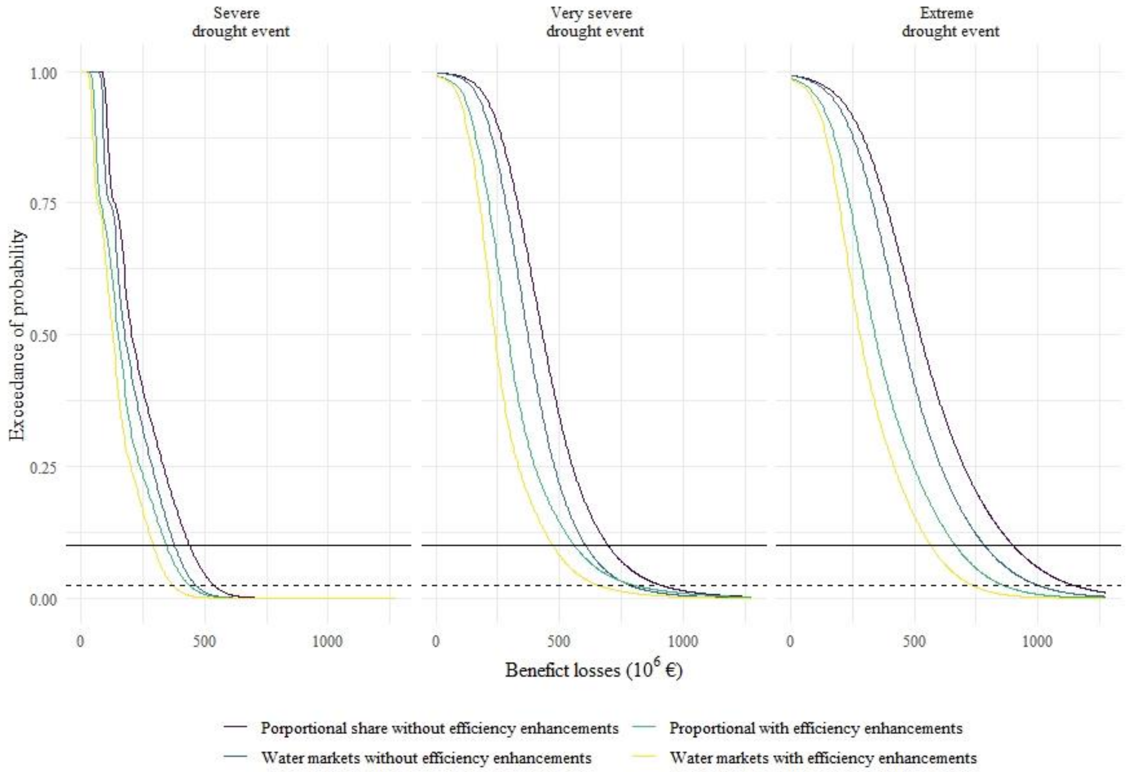

Figure A12. Conditional loss of benefits (10^6 €) by policy at quantiles 0.5, 0.9, 0.95 and 0.99.

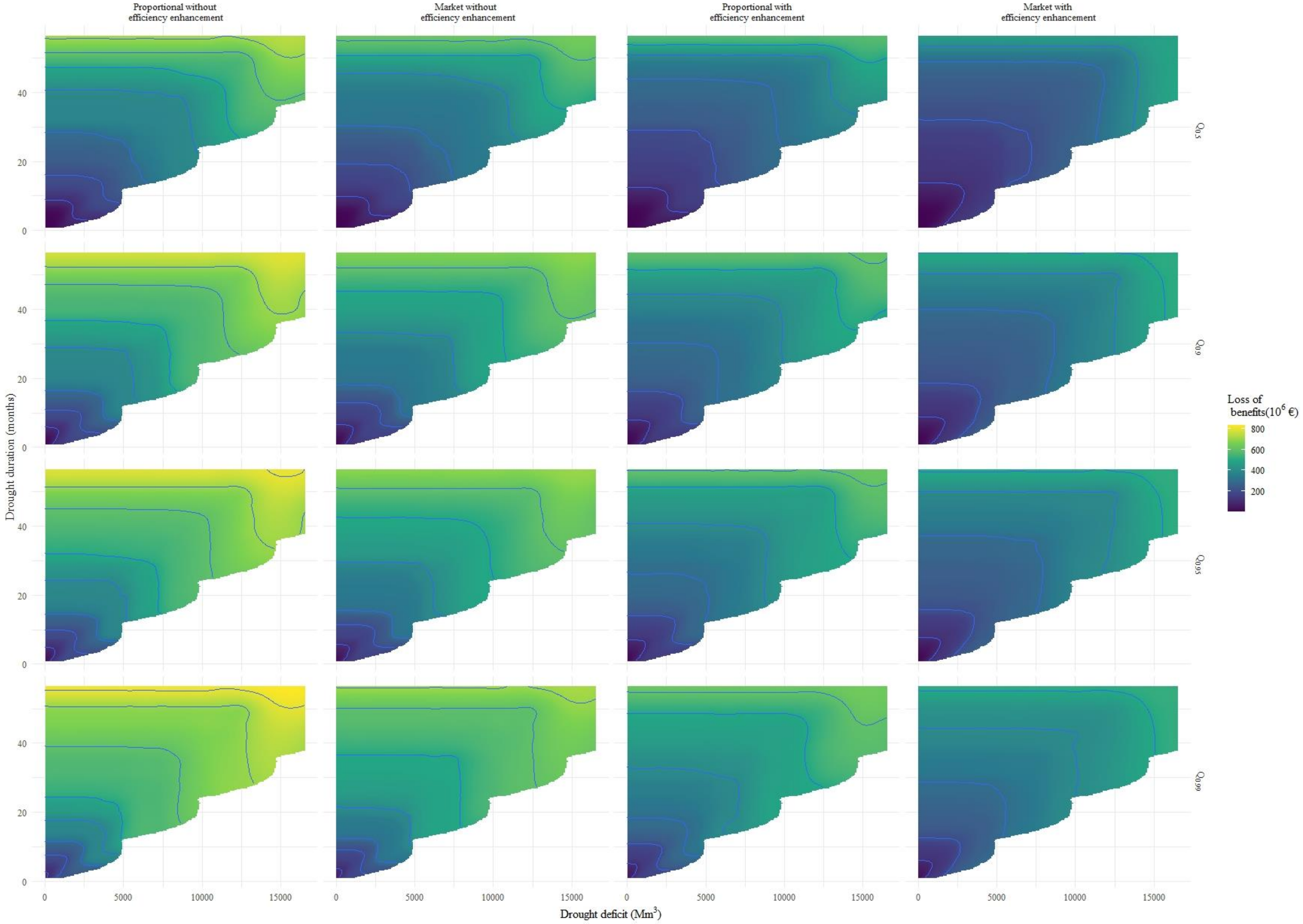

References

Aas, K., Czado, C., Frigessi, A., Bakken, H., 2009. Pair-copula constructions of multiple dependence. Insurance: Mathematics and Economics 44, 182–198. https://doi.org/10.1016/j.insmatheco.2007.02.001

Cribari-Neto, F., Zeileis, A., 2010. Beta Regression in R. J. Stat. Soft. 34. https://doi.org/10.18637/jss.v034.i02

Hayfield, T., Racine, J.S., 2008. Nonparametric Econometrics: The np Package. J. Stat. Soft. 27. https://doi.org/10.18637/jss.v027.i05

Ferrari, S., Cribari-Neto, F., 2004. Beta Regression for Modelling Rates and Proportions. Journal of Applied Statistics 31, 799–815. https://doi.org/10.1080/0266476042000214501

Li, Q., Lin, J., Racine, J.S., 2013. Optimal Bandwidth Selection for Nonparametric Conditional Distribution and Quantile Functions. Journal of Business & Economic Statistics 31, 57–65. https://doi.org/10.1080/07350015.2012.738955

Kraus, D., Czado, C., 2017. D-vine copula based quantile regression. Computational Statistics & Data Analysis 110, 1–18. https://doi.org/10.1016/j.csda.2016.12.009